

A SPACE–TIME TREFFTZ DISCONTINUOUS GALERKIN METHOD FOR THE LINEAR SCHRÖDINGER EQUATION *

SERGIO GÓMEZ[†] AND ANDREA MOIOLA[†]

Abstract. A space–time Trefftz discontinuous Galerkin method for the Schrödinger equation with piecewise-constant potential is proposed and analyzed. Following the spirit of Trefftz methods, trial and test spaces are spanned by non-polynomial complex wave functions that satisfy the Schrödinger equation locally on each element of the space–time mesh. This allows to significantly reduce the number of degrees of freedom in comparison with full polynomial spaces. We prove well-posedness and stability of the method, and, for the one- and two-dimensional cases, optimal, high-order, h -convergence error estimates in a skeleton norm. Some numerical experiments validate the theoretical results presented.

Key words. Linear Schrödinger equation; Trefftz method; discontinuous Galerkin method; *a priori* error estimate; h -convergence; non-polynomial basis functions.

AMS subject classifications. 65M60, 78M10, 35Q41

1. Introduction. In this work we consider the following initial boundary value problem for the homogeneous, time-dependent Schrödinger equation on a space–time cylinder $Q = \Omega \times I$, where Ω is an open and bounded domain in \mathbb{R}^d , $d \in \mathbb{N}$, with Lipschitz boundary $\partial\Omega$ and $I = (0, T)$, for some $T > 0$:

$$\begin{aligned} (1.1a) \quad & i \frac{\partial \psi}{\partial t} + \Delta \psi - V \psi = 0, \quad \text{in } Q, \\ (1.1b) \quad & \psi = g_D, \quad \text{on } \partial\Omega \times I, \\ (1.1c) \quad & \psi(\mathbf{x}, 0) = \psi_0(\mathbf{x}), \quad \text{on } \Omega. \end{aligned}$$

Here the Dirichlet boundary datum g_D and the initial condition ψ_0 are given functions; $V : \Omega \rightarrow \mathbb{R}$ is a piecewise-constant potential and the Laplacian operator Δ refers to the space variable \mathbf{x} only. Problem (1.1) is well-posed if, e.g., $\psi_0 \in H_0^1(\Omega)$ and $g_D = 0$, by [20, Chapter 3, Thm. 10.1, Rem. 10.2]; in this case $\psi \in C^0(0, T; H_0^1(\Omega)) \cap C^1(0, T; H^{-1}(\Omega))$.

The model (1.1) arises from a wide number of applications: it is the fundamental equation of quantum mechanics [19], in optics it is known as “paraxial wave equation” and approximates the Helmholtz equation when the optical field acts mostly along one specific axis (Fresnel’s approximation) [12], while in underwater acoustics it is called “parabolic equation” [18].

The aim of this work is to propose and analyze a space–time Trefftz-DG method for the numerical solution of (1.1). The main feature of Trefftz methods is that they seek approximations in spaces spanned by local solutions of the partial differential equation considered. This typically requires non-polynomial basis functions. Trefftz schemes are mainly motivated by their significant reduction in the computational cost and number of degrees of freedom with respect to traditional polynomial approximations, and by their effectiveness in dealing with the intrinsic highly oscillatory behavior

*

Funding: A. Moiola acknowledges support from GNCS–INDAM, from PRIN project “NA-FROM-PDEs” and from MIUR through the “Dipartimenti di Eccellenza” Program (2018–2022) — Dept. of Mathematics, University of Pavia.

[†]Dipartimento di Matematica “F. Casorati”, Università di Pavia, 27100 Pavia, Italy. (sergio.gomez01@universitadipavia.it, andrea.moiola@unipv.it).

in the solution of certain problems. On the other hand, Discontinuous Galerkin (DG) is a class of finite element methods that do not impose continuity in a strong sense on the approximation, making them specially suitable to be combined with Trefftz bases, which are naturally discontinuous.

Trefftz-DG methods have been successfully derived for many important equations; among others, the Helmholtz equation [11, 15], the time-harmonic and time-dependent Maxwell's equations [9, 14], the second- and first-order formulations of the acoustic wave equation [3, 23]. However, to the best of our knowledge, this is the first attempt to study the application of a Trefftz-DG method to the linear Schrödinger equation.

The well-posedness and quasi-optimality error analysis of the Trefftz-DG scheme closely follows the analysis previously developed for the wave [23, §5.2] and the Helmholtz [15, §2.2.1] equations. This part admits the use of any discrete Trefftz space. The chosen DG formulation admits general polytopic space meshes that are shape-regular and locally quasi-uniform. Inverse estimates are not needed in the analysis: this is a strong advantage in comparison to other DG formulations (such as interior-penalty, see [3] for a Trefftz example) because inverse estimates for non-polynomial discrete Trefftz spaces are in general hard to obtain (see [11, §3.2]).

Differently from the acoustic wave equation [23], the presence of derivatives of different orders in (1.1a) prevents the existence of non-trivial polynomial solutions of the Schrödinger equation, so we construct Trefftz basis functions as simple complex exponentials (4.1). In order to establish convergence rates in the mesh size h , the key ingredient is the analysis of the approximation properties of carefully designed discrete spaces. The key idea was introduced by O. Cessenat and B. Després in the proof of [7, Thm. 3.7] (in the case of the ultra weak variational formulation (UWVF) applied to the Helmholtz equation): given any smooth PDE solution ψ , if the local discrete space contains an element with the same degree- p Taylor polynomial of ψ , then the space enjoys the same h -approximation properties of the space \mathbb{P}^p of degree- p polynomials. We prove that this condition is satisfied by a simple discrete space \mathbb{T}^p in low space dimensions $d = 1, 2$. Additional difficulties are due to the fact that we only assume Sobolev regularity of the PDE solution, so the Taylor polynomial has to be understood in an “averaged” sense. It turns out that $\dim \mathbb{T}^p \ll \dim \mathbb{P}^p$: the Trefftz scheme allows much faster convergence in terms of degrees of freedom than classical polynomial DG schemes, see Remark 4.13. This approach to the Trefftz approximation theory is completely different from that used for the Helmholtz equation in [22], which is based on the use of an integral (Vekua) transform and circular wave expansions.

The paper is structured as follows: in Section 2 we introduce some standard notation and present the proposed Trefftz-DG method whose numerical fluxes are chosen as upwind in time and classical average in space with an appropriate complex penalization. In Section 3 we prove the well-posedness and quasi-optimality of the Trefftz-DG approximation for arbitrary dimensions and discrete Trefftz subspaces. Section 4 is devoted to the error analysis for discrete subspaces spanned by complex exponentials satisfying the Schrödinger equation. In Subsection 4.2 we present a condition which guarantees optimal local approximation of the exact solution in a general discrete Trefftz space; assuming that such condition is satisfied we prove an h -estimate in a mesh-skeleton norm in Subsection 4.5. In Subsections 4.3 and 4.4 we prove that the assumed condition is indeed true for the $(1+1)$ and $(2+1)$ dimensional cases under some restrictions of the tuning parameters for our basis choice. Some numerical experiments validating our theoretical results are presented in Section 5. We propose some possible future extensions of the method and its analysis in Section 6.

2. Trefftz-discontinuous Galerkin method.

2.1. Mesh and DG notation. Let the time interval $(0, T)$ be partitioned as

$$0 = t_0 < t_1 < \dots < t_N = T, \\ I_n := (t_{n-1}, t_n), \quad h_n := t_n - t_{n-1}, \quad h_t := \max_{1 \leq n \leq N} h_n.$$

We denote the time-slabs $D_n := \Omega \times I_n$. For each $n = 1, \dots, N$, we assume to have a polytopic partition $\mathcal{T}_{h_{\mathbf{x}}, n}^{\mathbf{x}} = \{K_{\mathbf{x}}\}$ of Ω such that for all $K_{\mathbf{x}} \in \mathcal{T}_{h_{\mathbf{x}}, n}^{\mathbf{x}}$, the restriction of the potential V to $K_{\mathbf{x}}$ is constant and

$$h_{K_{\mathbf{x}}} := \text{diam}(K_{\mathbf{x}}), \quad h_{\mathbf{x}} := \max_{K_{\mathbf{x}} \in \mathcal{T}_{h_{\mathbf{x}}, n}^{\mathbf{x}}, n=1, \dots, N} h_{K_{\mathbf{x}}}.$$

Additionally we also assume that each $\mathcal{T}_{h_{\mathbf{x}}, n}^{\mathbf{x}}$ satisfies the following properties:

- **Shape-regularity:** there exists a number $\text{sr}(\mathcal{T}_h) > 0$ such that $h_{K_{\mathbf{x}}} \leq \rho_{K_{\mathbf{x}}} \text{sr}(\mathcal{T}_h)$ for all elements $K_{\mathbf{x}} \in \mathcal{T}_{h_{\mathbf{x}}, n}^{\mathbf{x}}$, where $\rho_{K_{\mathbf{x}}}$ is the radius of a d -dimensional ball contained in $K_{\mathbf{x}}$.
- **Local quasi-uniformity in space:** there exists a number $\text{lqu}(\mathcal{T}_h) > 0$ such that $h_{K_{\mathbf{x}}^1} \leq h_{K_{\mathbf{x}}^2} \text{lqu}(\mathcal{T}_h)$ for all $n = 1, \dots, N$ and $K_{\mathbf{x}}^1, K_{\mathbf{x}}^2 \in \mathcal{T}_{h_{\mathbf{x}}, n}^{\mathbf{x}}$ such that $K_{\mathbf{x}}^1 \cap K_{\mathbf{x}}^2$ has positive $(d-1)$ -dimensional measure.

We define the space-time finite element mesh

$$\mathcal{T}_h(Q) := \left\{ K = K_{\mathbf{x}} \times I_n : K_{\mathbf{x}} \in \mathcal{T}_{h_{\mathbf{x}}, n}^{\mathbf{x}}, n = 1, \dots, N \right\}.$$

Each internal mesh face F (i.e. any $F = \partial K_1 \cap \partial K_2$, for $K_1, K_2 \in \mathcal{T}_h(Q)$, with positive d -dimensional measure) is either

$$\begin{cases} \text{a space-like face:} & \text{if } F \subset \Omega \times \{t_n\}, \text{ for } 0 < n < N, \text{ or} \\ \text{a time-like face:} & \text{if } F \subset \partial(K_{\mathbf{x}}^1 \times I_n) \cap \partial(K_{\mathbf{x}}^2 \times I_n), \\ & \text{for } K_{\mathbf{x}}^1, K_{\mathbf{x}}^2 \in \mathcal{T}_{h_{\mathbf{x}}, n}^{\mathbf{x}}, 1 \leq n \leq N. \end{cases}$$

We denote the mesh skeleton and its parts as

$$\mathcal{F}_h := \bigcup_{K \in \mathcal{T}_h(Q)} \partial K, \quad \mathcal{F}_h^0 := \Omega \times \{0\}, \quad \mathcal{F}_h^T := \Omega \times \{T\}, \quad \mathcal{F}_h^D := \partial \Omega \times (0, T),$$

$\mathcal{F}_h^{\text{time}}$:= the union of all the time-like faces,

$\mathcal{F}_h^{\text{space}}$:= the union of all the space-like faces.

We also employ the standard DG notation for the averages $\{\{\cdot\}\}$ and space $[\![\cdot]\!]_{\mathbf{N}}$ and time $[\![\cdot]\!]_t$ jumps for piecewise-continuous complex scalar w and vector $\boldsymbol{\tau}$ fields:

$$\begin{cases} \{\{w\}\} := \frac{1}{2}(w|_{K_1} + w|_{K_2}) & \text{on } \partial K_1 \cap \partial K_2 \subset \mathcal{F}_h^{\text{time}}, \\ \{\{\boldsymbol{\tau}\}\} := \frac{1}{2}(\boldsymbol{\tau}|_{K_1} + \boldsymbol{\tau}|_{K_2}) & \\ \llbracket w \rrbracket_{\mathbf{N}} := w|_{K_1} \mathbf{n}_{K_1}^x + w|_{K_2} \mathbf{n}_{K_2}^x & \text{on } \partial K_1 \cap \partial K_2 \subset \mathcal{F}_h^{\text{time}}, \\ \llbracket \boldsymbol{\tau} \rrbracket_{\mathbf{N}} := \boldsymbol{\tau}|_{K_1} \cdot \mathbf{n}_{K_1}^x + \boldsymbol{\tau}|_{K_2} \cdot \mathbf{n}_{K_2}^x & \\ \llbracket w \rrbracket_t := w^- - w^+ & \text{on } \mathcal{F}_h^{\text{space}}, \\ \llbracket \boldsymbol{\tau} \rrbracket_t := \boldsymbol{\tau}^- - \boldsymbol{\tau}^+, & \end{cases}$$

where $\vec{\mathbf{n}}_K^x \in \mathbb{R}^d$ is the space component of the outward-pointing unit normal vector on $\partial K \cap \mathcal{F}_h^{\text{time}}$, and the superscripts “−” and “+” are used to denote the traces on $\Omega \times \{t_n\}$ of scalar and vector fields from the time-slabs D_n and D_{n+1} , at lower and higher times, respectively.

2.2. Formulation of the Trefftz-DG method. We define the local and global Trefftz spaces:

$$(2.1) \quad \begin{aligned} \mathbf{T}(K) &:= \left\{ w \in H^1(I_n; L^2(K_{\mathbf{x}})) \cap L^2(I_n; H^2(K_{\mathbf{x}})) \text{ such that} \right. \\ &\quad \left. i \frac{\partial w}{\partial t} + \Delta w - Vw = 0 \text{ on } K = K_{\mathbf{x}} \times I_n \right\}, \\ \mathbf{T}(\mathcal{T}_h) &:= \left\{ w \in L^2(Q)^{d+1} \mid w|_K \in \mathbf{T}(K), \forall K \in \mathcal{T}_h(Q) \right\}. \end{aligned}$$

For any finite-dimensional subspace $\mathbb{T}_p(\mathcal{T}_h) \subset \mathbf{T}(\mathcal{T}_h)$ the proposed Trefftz-DG method applied to (1.1) seeks an approximation $\psi_{hp}(\mathbf{x}, t) \in \mathbb{T}_p(\mathcal{T}_h)$ of the exact solution $\psi(\mathbf{x}, t) \in \mathbf{T}(\mathcal{T}_h)$ such that for any test function $s_{hp} \in \mathbb{T}_p(\mathcal{T}_h)$ the following equation is satisfied for all $K \in \mathcal{T}_h(Q)$

$$(2.2) \quad \begin{aligned} &\int_K \psi_{hp} \left(i \overline{\frac{\partial s_{hp}}{\partial t} + \Delta s_{hp} - V s_{hp}} \right) dV \\ &+ \oint_{\partial K} \left[i \widehat{\psi}_{hp} \overline{s_{hp}} n_K^t + \left(\widehat{\nabla} \psi_{hp} \overline{s_{hp}} - \widehat{\psi}_{hp} \nabla s_{hp} \right) \cdot \vec{\mathbf{n}}_K^x \right] dS = 0, \end{aligned}$$

where $\bar{\cdot}$ denotes the complex conjugate, n_K^t is the time component of the outward-pointing unit normal vector on ∂K (so $n_K^t = \pm 1$ on $\partial K \cap (\mathcal{F}_h^{\text{space}} \cup \mathcal{F}_h^0 \cup \mathcal{F}_h^T)$ and $n_K^t = 0$ otherwise). Equation (2.2) is obtained integrating by parts the product of (1.1a) and $\overline{s_{hp}}$ twice in space and once in time, noting the sign change in the time-derivative term due to the conjugation of i . The so-called *numerical fluxes* $\widehat{\psi}_{hp}$ and $\widehat{\nabla} \psi_{hp}$ are approximations of the traces of ψ_{hp} and $\nabla \psi_{hp}$ on \mathcal{F}_h . We choose them as:

$$\begin{aligned} \widehat{\psi}_{hp} &:= \begin{cases} \psi_{hp}^-, & \text{on } \mathcal{F}_h^{\text{space}}, \\ \psi_{hp}, & \text{on } \mathcal{F}_h^T, \\ \psi_0, & \text{on } \mathcal{F}_h^0, \\ \{\{\psi_{hp}\}\} - i\beta \llbracket \nabla \psi_{hp} \rrbracket_{\mathbf{N}}, & \text{on } \mathcal{F}_h^{\text{time}}, \\ g_D, & \text{on } \mathcal{F}_h^D, \end{cases} \\ \widehat{\nabla} \psi_{hp} &:= \begin{cases} \{\{\nabla \psi_{hp}\}\} + i\alpha \llbracket \psi_{hp} \rrbracket_{\mathbf{N}}, & \text{on } \mathcal{F}_h^{\text{time}}, \\ \nabla \psi_{hp} + i\alpha (\psi_{hp} - g_D) \vec{\mathbf{n}}_{\Omega}^x, & \text{on } \mathcal{F}_h^D, \end{cases} \end{aligned}$$

where $\alpha \in L^\infty(\mathcal{F}_h^{\text{time}} \cup \mathcal{F}_h^D)$ and $\beta \in L^\infty(\mathcal{F}_h^{\text{time}})$ are some mesh-dependent stabilization parameters with $\text{ess inf}_{\mathcal{F}_h^{\text{time}} \cup \mathcal{F}_h^D} \alpha > 0$ and $\text{ess inf}_{\mathcal{F}_h^{\text{time}}} \beta > 0$.

Since all $s_{hp} \in \mathbb{T}_p(\mathcal{T}_h)$ satisfy (1.1a) in each mesh element, the volume integral in Equation (2.2) vanishes and thus the Trefftz-DG method only involves integrals on the mesh skeleton. Consequently, after summing Equation (2.2) over all the elements $K \in \mathcal{T}_h(Q)$ and substituting the definition of the numerical fluxes, the following Trefftz-DG variational formulation is obtained:

$$(2.3) \quad \text{Seek } \psi_{hp} \in \mathbb{T}_p(\mathcal{T}_h) \text{ such that: } \mathcal{A}(\psi_{hp}; s_{hp}) = \ell(s_{hp}), \quad \forall s_{hp} \in \mathbb{T}_p(\mathcal{T}_h),$$

where

$$\begin{aligned} \mathcal{A}(\psi_{hp}; s_{hp}) &:= \int_{\mathcal{F}_h^{\text{space}}} i\psi_{hp}^- \llbracket \overline{s_{hp}} \rrbracket_t \, d\mathbf{x} + \int_{\mathcal{F}_h^T} i\psi_{hp} \overline{s_{hp}} \, d\mathbf{x} \\ &+ \int_{\mathcal{F}_h^{\text{time}}} \left(\{\{\nabla\psi_{hp}\}\} \cdot \llbracket \overline{s_{hp}} \rrbracket_{\mathbf{N}} + i\alpha \llbracket \psi_{hp} \rrbracket_{\mathbf{N}} \cdot \llbracket \overline{s_{hp}} \rrbracket_{\mathbf{N}} - \{\{\psi_{hp}\}\} \llbracket \nabla \overline{s_{hp}} \rrbracket_{\mathbf{N}} \right. \\ &\quad \left. + i\beta \llbracket \nabla\psi_{hp} \rrbracket_{\mathbf{N}} \llbracket \nabla \overline{s_{hp}} \rrbracket_{\mathbf{N}} \right) dS + \int_{\mathcal{F}_h^{\text{D}}} (\nabla\psi_{hp} \cdot \vec{\mathbf{n}}_{\Omega}^x + i\alpha\psi_{hp}) \overline{s_{hp}} \, dS, \\ \ell(s_{hp}) &:= \int_{\mathcal{F}_h^0} i\psi_0 \overline{s_{hp}} \, d\mathbf{x} + \int_{\mathcal{F}_h^{\text{D}}} g_{\text{D}} (\nabla \overline{s_{hp}} \cdot \vec{\mathbf{n}}_{\Omega}^x + i\alpha \overline{s_{hp}}) \, dS. \end{aligned}$$

3. Well-posedness, stability and quasi-optimality of the Trefftz-DG method. The theoretical results in this section are derived for arbitrary space dimension d and are independent of the specific discrete subspace $\mathbb{T}_p(\mathcal{T}_h)$ chosen.

The following identities will be used

$$(3.1a) \quad \operatorname{Re} (w^- \llbracket \overline{w} \rrbracket_t) - \frac{1}{2} \llbracket |w|^2 \rrbracket_t = \frac{1}{2} \llbracket |w|_t \rrbracket_t^2, \quad \text{on } \mathcal{F}_h^{\text{space}},$$

$$(3.1b) \quad \{\{w\}\} \llbracket \boldsymbol{\tau} \rrbracket_{\mathbf{N}} + \{\{\boldsymbol{\tau}\}\} \cdot \llbracket w \rrbracket_{\mathbf{N}} = \llbracket w \boldsymbol{\tau} \rrbracket_{\mathbf{N}}, \quad \text{on } \mathcal{F}_h^{\text{time}}.$$

Recalling that the numerical flux parameters α and β are positive, we define the following mesh-dependent semi-norms:

$$\begin{aligned} (3.2) \quad |||w|||_{\text{DG}}^2 &:= \llbracket [w]_t \rrbracket_{L^2(\mathcal{F}_h^{\text{space}})}^2 + \frac{1}{2} \|w\|_{L^2(\mathcal{F}_h^T \cup \mathcal{F}_h^0)}^2 + \left\| \alpha^{1/2} w \right\|_{L^2(\mathcal{F}_h^{\text{D}})}^2 \\ &\quad + \left\| \alpha^{1/2} \llbracket w \rrbracket_{\mathbf{N}} \right\|_{L^2(\mathcal{F}_h^{\text{time}})^d}^2 + \left\| \beta^{1/2} \llbracket \nabla w \rrbracket_{\mathbf{N}} \right\|_{L^2(\mathcal{F}_h^{\text{time}})}^2, \\ |||w|||_{\text{DG}^+}^2 &:= |||w|||_{\text{DG}}^2 + \|w^-\|_{L^2(\mathcal{F}_h^{\text{space}})}^2 + \left\| \alpha^{-1/2} \{\{\nabla w\}\} \right\|_{L^2(\mathcal{F}_h^{\text{time}})^d}^2 \\ &\quad + \left\| \alpha^{-1/2} \nabla w \cdot \vec{\mathbf{n}}_{\Omega}^x \right\|_{L^2(\mathcal{F}_h^{\text{D}})}^2 + \left\| \beta^{-1/2} \{\{w\}\} \right\|_{L^2(\mathcal{F}_h^{\text{time}})}^2. \end{aligned}$$

Even though $|||\cdot|||_{\text{DG}}$ and $|||\cdot|||_{\text{DG}^+}$ are just seminorms on $H^1(\mathcal{T}_h)$, the following lemma shows that they are indeed norms on $\mathbf{T}(\mathcal{T}_h)$. Furthermore, continuity and coercivity of the sesquilinear form $\mathcal{A}(\cdot; \cdot)$ with respect to these norms are proven in [Propositions 3.2](#) and [3.3](#).

LEMMA 3.1. $|||\cdot|||_{\text{DG}}$ and $|||\cdot|||_{\text{DG}^+}$ are norms on $\mathbf{T}(\mathcal{T}_h)$.

Proof. It is enough to prove that $|||v|||_{\text{DG}} = 0$, $v \in \mathbf{T}(\mathcal{T}_h)$, implies $v = 0$. Indeed, if $|||v|||_{\text{DG}} = 0$, then, by the definitions [\(2.1\)](#) and [\(3.2\)](#) of the Trefftz space and the DG norm, $v \in H^1(0, T; L^2(\Omega)) \cap L^2(0, T; H_0^1(\Omega))$. Then, for all w in the same space,

$$0 = \sum_{K \in \mathcal{T}_h} \int_K \left(i \frac{\partial v}{\partial t} + \Delta v - Vv \right) \overline{w} \, dV = \int_Q \left(i \frac{\partial v}{\partial t} \overline{w} - \nabla v \cdot \nabla \overline{w} - Vv \overline{w} \right) dV$$

by the Trefftz property, where the boundary terms on $\mathcal{F}_h^{\text{time}}$ arising from the integration by parts cancel because $\llbracket \nabla v \rrbracket_{\mathbf{N}} = 0$ is implied by $|||v|||_{\text{DG}} = 0$. Moreover $v(\cdot, 0) = 0$. This means that v is variational solution of the homogeneous Schrödinger problem [\(1.1\)](#) (i.e. with $g_{\text{D}} = 0$ and $\psi_0 = 0$). By the uniqueness of the solution in [\[20, Chapter 3, Thm. 10.1\]](#), it follows that $v = 0$. \square

PROPOSITION 3.2 (Coercivity). *For all $w \in \mathbf{T}(\mathcal{T}_h)$ the following identity holds*

$$(3.3) \quad \operatorname{Im}(\mathcal{A}(w; w)) = \|w\|_{\text{DG}}^2.$$

Proof. Elementwise integration by parts for $w \in \mathbf{T}(\mathcal{T}_h)$ gives the identity:

$$(3.4) \quad \begin{aligned} 0 &= \operatorname{Im} \left(\sum_{K \in \mathcal{T}_h(Q)} \int_K w \overline{\left(i \frac{\partial w}{\partial t} + \Delta w - Vw \right)} dV \right) \\ &= -\frac{1}{2} \sum_{K \in \mathcal{T}_h(Q)} \int_K \frac{\partial |w|^2}{\partial t} dV + \operatorname{Im} \left(\int_{\mathcal{F}_h^{\text{time}}} \llbracket w \nabla \bar{w} \rrbracket_{\mathbf{N}} dS + \int_{\mathcal{F}_h^{\text{D}}} w \nabla \bar{w} \cdot \bar{\mathbf{n}}_{\Omega}^x dS \right) \\ &= -\frac{1}{2} \left(\int_{\mathcal{F}_h^{\text{space}}} \left[\left[|w|^2 \right] \right]_t d\mathbf{x} + \int_{\mathcal{F}_h^T} |w|^2 d\mathbf{x} - \int_{\mathcal{F}_h^0} |w|^2 d\mathbf{x} \right) \\ &\quad + \operatorname{Im} \left(\int_{\mathcal{F}_h^{\text{time}}} \llbracket w \nabla \bar{w} \rrbracket_{\mathbf{N}} dS + \int_{\mathcal{F}_h^{\text{D}}} w \nabla \bar{w} \cdot \bar{\mathbf{n}}_{\Omega}^x dS \right). \end{aligned}$$

Together with the jump identities in (3.1), this gives

$$\begin{aligned} \operatorname{Im}(\mathcal{A}(w; w)) &= \operatorname{Im} \left(\mathcal{A}(w; w) + \sum_{K \in \mathcal{T}_h(Q)} \int_K w \overline{\left(i \frac{\partial w}{\partial t} + \Delta w - Vw \right)} dV \right) \\ &\stackrel{(3.4)}{=} \int_{\mathcal{F}_h^{\text{space}}} \left(\operatorname{Re} \left(w^- \llbracket \bar{w} \rrbracket_t \right) - \frac{1}{2} \left[\left[|w|^2 \right] \right]_t \right) d\mathbf{x} \\ &\quad + \frac{1}{2} \left(\int_{\mathcal{F}_h^T} |w|^2 d\mathbf{x} + \int_{\mathcal{F}_h^0} |w|^2 d\mathbf{x} \right) + \int_{\mathcal{F}_h^{\text{D}}} \alpha |w|^2 dS \\ &\quad + \int_{\mathcal{F}_h^{\text{time}}} \left(\alpha \llbracket [w] \rrbracket_{\mathbf{N}}^2 + \beta \llbracket [\nabla w] \rrbracket_{\mathbf{N}}^2 \right) dS \\ &\quad + \int_{\mathcal{F}_h^{\text{time}}} \operatorname{Im} \left(\{ \{ \nabla w \} \} \cdot \llbracket \bar{w} \rrbracket_{\mathbf{N}} - \{ \{ w \} \} \llbracket [\nabla \bar{w}] \rrbracket_{\mathbf{N}} + \llbracket [w \nabla \bar{w}] \rrbracket_{\mathbf{N}} \right) dS \\ &\stackrel{(3.1)}{=} \|w\|_{\text{DG}}^2. \quad \square \end{aligned}$$

PROPOSITION 3.3 (Continuity). *The sesquilinear form $\mathcal{A}(\cdot; \cdot)$ and the linear functional $\ell(\cdot)$ are continuous in the following sense:*

$$(3.5a) \quad |\mathcal{A}(v; w)| \leq 2 \|v\|_{\text{DG}^+} \|w\|_{\text{DG}}, \quad \forall v, w \in \mathbf{T}(\mathcal{T}_h),$$

$$(3.5b) \quad |\ell(v)| \leq \left(2 \|\psi_0\|_{L^2(\mathcal{F}_h^0)}^2 + 2 \left\| \alpha^{1/2} g_{\text{D}} \right\|_{L^2(\mathcal{F}_h^{\text{D}})}^2 \right)^{1/2} \|w\|_{\text{DG}^+}, \quad \forall v \in \mathbf{T}(\mathcal{T}_h).$$

Furthermore, if $g_{\text{D}} = 0$, then $|\ell(v)| \leq \sqrt{2} \|\psi_0\|_{L^2(\mathcal{F}_h^0)} \|w\|_{\text{DG}}$.

Proof. Let $v, w \in \mathbf{T}(\mathcal{T}_h)$. After applying the triangle and the Cauchy-Schwarz inequalities several times we obtain

$$\begin{aligned} |\mathcal{A}(v; w)| &\leq \|v^-\|_{L^2(\mathcal{F}_h^{\text{space}})} \left\| \llbracket [w] \rrbracket_t \right\|_{L^2(\mathcal{F}_h^{\text{space}})} + \|v\|_{L^2(\mathcal{F}_h^T)} \|w\|_{L^2(\mathcal{F}_h^T)} \\ &\quad + \left(\left\| \alpha^{-\frac{1}{2}} \nabla v \cdot \bar{\mathbf{n}}_{\Omega}^x \right\|_{L^2(\mathcal{F}_h^{\text{D}})} + \left\| \alpha^{\frac{1}{2}} v \right\|_{L^2(\mathcal{F}_h^{\text{D}})} \right) \left\| \alpha^{\frac{1}{2}} w \right\|_{L^2(\mathcal{F}_h^{\text{D}})} \\ &\quad + \left(\left\| \alpha^{-\frac{1}{2}} \{ \{ \nabla v \} \} \right\|_{L^2(\mathcal{F}_h^{\text{time}})_d} + \left\| \alpha^{\frac{1}{2}} \llbracket [v] \rrbracket_{\mathbf{N}} \right\|_{L^2(\mathcal{F}_h^{\text{time}})_d} \right) \left\| \alpha^{\frac{1}{2}} \llbracket [w] \rrbracket_{\mathbf{N}} \right\|_{L^2(\mathcal{F}_h^{\text{time}})_d} \end{aligned}$$

$$+ \left(\left\| \beta^{-\frac{1}{2}} \{v\} \right\|_{L^2(\mathcal{F}_h^{\text{time}})} + \left\| \beta^{\frac{1}{2}} \llbracket \nabla v \rrbracket_{\mathbf{N}} \right\|_{L^2(\mathcal{F}_h^{\text{time}})} \right) \left\| \beta^{\frac{1}{2}} \llbracket \nabla w \rrbracket_{\mathbf{N}} \right\|_{L^2(\mathcal{F}_h^{\text{time}})}.$$

Bound (3.5a) is then obtained by using Cauchy–Schwarz inequality once again. The bounds for the linear operator $\ell(\cdot)$ can be obtained in a similar way. \square

The following well-posedness and quasi-optimality theorem is a direct consequence of the Lax–Milgram theorem and [Propositions 3.2](#) and [3.3](#).

THEOREM 3.4 (Quasi-optimality). *For any finite-dimensional subspace $\mathbb{T}_p(\mathcal{T}_h)$ of $\mathbf{T}(\mathcal{T}_h)$ there exists a unique solution $\psi_{hp} \in \mathbb{T}_p(\mathcal{T}_h)$ satisfying (2.3). Furthermore, the following quasi-optimality condition holds:*

$$(3.6) \quad \|\psi - \psi_{hp}\|_{\text{DG}} \leq 3 \inf_{s_{hp} \in \mathbb{T}_p(\mathcal{T}_h)} \|\psi - s_{hp}\|_{\text{DG}+}.$$

[Theorem 3.4](#) allows to obtain an estimate of the error in the mesh-skeleton norm $\|\cdot\|_{\text{DG}}$ by studying the best approximation of the exact solution in $\mathbb{T}_p(\mathcal{T}_h)$ in the (slightly stronger) $\|\cdot\|_{\text{DG}+}$ norm; this is the subject of the next section.

Remark 3.5 (Error bounds at time t_n). [Theorem 3.4](#) allows to control the $L^2(\Omega)$ norm of the Galerkin error at final time $t = T$, but only the L^2 norm of the time jump $\llbracket \psi - \psi_{hp} \rrbracket_t$ on each space-like mesh interface $\Omega \times \{t_n\}$ (recall the definition of the $\|\cdot\|_{\text{DG}}$ norm (3.2)). However, a similar bound on the stronger error norm $\|\psi^- - \psi_{hp}^-\|_{L^2(\Omega \times \{t_n\})}$, involving only the trace of the error from the time-slab $D_n = \Omega \times (t_{n-1}, t_n)$, can be obtained by extending the argument of this section to the partial cylinder $\Omega \times (0, t_n)$ (as opposed to the full cylinder Q), precisely as in [[23](#), Prop. 1].

Remark 3.6 (Energy dissipation). It follows from integration by parts that [Equation \(1.1\)](#) with homogeneous boundary conditions $g_{\text{D}} = 0$ preserves the energy (or probability) functional $\mathcal{E}(t; \psi) := \frac{1}{2} \int_{\Omega} |\psi(\mathbf{x}, t)|^2 \, d\mathbf{x}$, i.e. $\frac{d}{dt} \mathcal{E}(t; \psi) = 0$. Unfortunately, the Trefftz-DG method is not conservative. However, as in the case of the acoustic wave equation [[23](#), §5.3], it is dissipative and the energy loss can be quantified in terms of the initial condition error, the jumps of the solution on the mesh skeleton and the error on \mathcal{F}_h^{D} due to the weak imposition of the boundary conditions, which, as stated in [Remark 4.12](#), all converge to zero as we refine the space–time mesh. More precisely, for $g_{\text{D}} = 0$ the Trefftz-DG solution of (2.3) satisfies

$$\begin{aligned} \mathcal{E}(0; \psi_0) - \mathcal{E}(T; \psi_{hp}) &= \mathcal{E}_{\text{loss}} := \delta_{\mathcal{E}} + \frac{1}{2} \|\psi_0 - \psi_{hp}\|_{\mathcal{F}_h^0}^2, \\ \delta_{\mathcal{E}} &:= \|\llbracket \psi_{hp} \rrbracket_t\|_{L^2(\mathcal{F}_h^{\text{space}})}^2 + \left\| \alpha^{1/2} \psi_{hp} \right\|_{L^2(\mathcal{F}_h^{\text{D}})}^2 \\ &\quad + \left\| \alpha^{1/2} \llbracket \psi_{hp} \rrbracket_{\mathbf{N}} \right\|_{L^2(\mathcal{F}_h^{\text{time}})_d}^2 + \left\| \beta^{1/2} \llbracket \nabla \psi_{hp} \rrbracket_{\mathbf{N}} \right\|_{L^2(\mathcal{F}_h^{\text{time}})}^2. \end{aligned}$$

This follows from the definition of the $\|\cdot\|_{\text{DG}}$ norm of the solution ψ_h , the coercivity of the sesquilinear form $\mathcal{A}(\cdot; \cdot)$, the definition of $\ell(\cdot)$ and simple manipulations:

$$\begin{aligned} \mathcal{E}(0; \psi_{hp}) + \mathcal{E}(T; \psi_{hp}) + \delta_{\mathcal{E}} &\stackrel{(3.2)}{=} \|\psi_{hp}\|_{\text{DG}}^2 \stackrel{(3.3)}{=} \text{Im}(\mathcal{A}(\psi_{hp}; \psi_h)) \stackrel{(2.3)}{=} \text{Im}(\ell(\psi_{hp})) \\ &\stackrel{(g_{\text{D}}=0)}{=} \text{Re} \int_{\mathcal{F}_h^0} \psi_0 \overline{\psi_{hp}} \, d\mathbf{x} = \mathcal{E}(0; \psi_0) + \mathcal{E}(0; \psi_{hp}) - \frac{1}{2} \|\psi_0 - \psi_{hp}\|_{\mathcal{F}_h^0}^2. \end{aligned}$$

Further manipulations give the identity $\mathcal{E}_{\text{loss}} = \|\psi - \psi_{hp}\|_{\text{DG}}^2 - \mathcal{E}(T, \psi - \psi_{hp})$.

Remark 3.7. We briefly explain how to modify the method to allow other boundary conditions. Let $\partial\Omega \times I$ be partitioned in three parts with Dirichlet, Neumann and Robin conditions:

$$\begin{aligned} \psi &= g_D && \text{on } \mathcal{F}_h^D = \Gamma_D \times I, \\ \nabla\psi \cdot \mathbf{n}_\Omega^x &= g_N && \text{on } \mathcal{F}_h^N = \Gamma_N \times I, \\ \nabla\psi \cdot \mathbf{n}_\Omega^x - i\vartheta\psi &= g_R && \text{on } \mathcal{F}_h^R = \Gamma_R \times I, \end{aligned}$$

for some positive ‘‘impedance’’ function $\vartheta \in L^\infty(\mathcal{F}_h^R)$. We extend the numerical flux parameter β to $\mathcal{F}_h^{\text{time}} \cup \mathcal{F}_h^N$, fix a function δ on \mathcal{F}_h^R such that $0 < \delta < 1$ and choose the numerical fluxes on $\partial\Omega \times I$ as

$$\widehat{\psi}_{hp} := \begin{cases} g_D, & \text{on } \mathcal{F}_h^D, \\ \psi_{hp} - i\beta(\nabla\psi_{hp} \cdot \mathbf{n}_\Omega^x - g_N), & \text{on } \mathcal{F}_h^N, \\ \psi_{hp} + \delta(i\vartheta)^{-1}(\nabla\psi_{hp} \cdot \mathbf{n}_\Omega^x - i\vartheta\psi_{hp} - g_R), & \text{on } \mathcal{F}_h^R, \end{cases}$$

$$\widehat{\nabla\psi}_{hp} \cdot \mathbf{n}_\Omega^x := \begin{cases} \nabla\psi_{hp} \cdot \mathbf{n}_\Omega^x + i\alpha(\psi_{hp} - g_D), & \text{on } \mathcal{F}_h^D, \\ g_N, & \text{on } \mathcal{F}_h^N, \\ \nabla\psi_{hp} \cdot \mathbf{n}_\Omega^x - (1 - \delta)(\nabla\psi_{hp} \cdot \mathbf{n}_\Omega^x - i\vartheta\psi_{hp} - g_R), & \text{on } \mathcal{F}_h^R. \end{cases}$$

This amounts to adding the following boundary terms to $\mathcal{A}(\psi_{hp}; s_{hp})$ and $\ell(s_{hp})$ in (2.3), respectively:

$$\begin{aligned} &\bullet \int_{\mathcal{F}_h^N} (-\psi_{hp} \nabla \overline{s_{hp}} \cdot \mathbf{n}_\Omega^x + i\beta(\nabla\psi_{hp} \cdot \mathbf{n}_\Omega^x)(\nabla \overline{s_{hp}} \cdot \mathbf{n}_\Omega^x)) \, dS \\ &\quad + \int_{\mathcal{F}_h^R} \left(\delta \nabla\psi_{hp} \cdot \mathbf{n}_\Omega^x + (1 - \delta)i\vartheta\psi_{hp} \right) \left(\overline{s_{hp}} + \frac{i}{\vartheta} \nabla \overline{s_{hp}} \cdot \mathbf{n}_\Omega^x \right) \, dS, \\ &\bullet \int_{\mathcal{F}_h^N} g_N (-\overline{s_{hp}} + i\beta \nabla \overline{s_{hp}} \cdot \mathbf{n}_\Omega^x) \, dS + \int_{\mathcal{F}_h^R} g_R \left((\delta - 1) \overline{s_{hp}} + \frac{i\delta}{\vartheta} \nabla \overline{s_{hp}} \cdot \mathbf{n}_\Omega^x \right) \, dS. \end{aligned}$$

In (3.2) both norms $|||\psi_{hp}|||_{\text{DG}}^2$ and $|||\psi_{hp}|||_{\text{DG}^+}^2$ have to be supplemented by the terms

$$\left\| \beta^{1/2} \nabla\psi_{hp} \cdot \mathbf{n}_\Omega^x \right\|_{L_2(\mathcal{F}_h^N)}^2 + \left\| (\vartheta(1 - \delta))^{1/2} \psi_{hp} \right\|_{L_2(\mathcal{F}_h^R)}^2 + \left\| (\delta\vartheta^{-1})^{1/2} \nabla\psi_{hp} \cdot \mathbf{n}_\Omega^x \right\|_{L_2(\mathcal{F}_h^R)}^2,$$

and a further term $\|\beta^{-1/2}\psi_{hp}\|_{L_2(\mathcal{F}_h^N)}^2$ has to be added to $|||\psi_{hp}|||_{\text{DG}^+}^2$. If $\mathcal{F}_h^R \neq \emptyset$, the continuity constant 2 of the sesquilinear form $\mathcal{A}(\cdot; \cdot)$ in Proposition 3.3 becomes

$$2 \max \left\{ \left\| \left(\frac{1 - \delta}{\delta} \right)^{1/2} \right\|_{L_\infty(\mathcal{F}_h^R)}, \left\| \left(\frac{\delta}{1 - \delta} \right)^{1/2} \right\|_{L_\infty(\mathcal{F}_h^R)} \right\}.$$

Then the a priori analysis carried out in this section can be extended to this setting.

4. Approximation and convergence analysis of the Trefftz-DG method.

In this section we prove h -estimates on the $|||\cdot|||_{\text{DG}^+}$ norm of the best approximation error of Schrödinger solutions by discrete Trefftz functions in $\mathbb{T}_p(\mathcal{T}_h) = \prod_{K \in \mathcal{T}_h(Q)} \mathbb{T}_p(K)$. The local space $\mathbb{T}_p(K)$ is defined for each $K = K_{\mathbf{x}} \times I_n \in \mathcal{T}_h(Q)$ and for $p \in \mathbb{N}$ as the following set of complex exponentials:

$$(4.1) \quad \mathbb{T}_p(K) := \text{span} \{ \phi_\ell(\mathbf{x}, t), \ell = 1, \dots, n_{d,p} \}, \quad \text{where}$$

$$\phi_\ell(\mathbf{x}, t) := \exp \left[i \left(k_\ell \mathbf{d}_\ell^\top \mathbf{x} - (k_\ell^2 + V|_K)t \right) \right] \quad \text{for } \ell = 1, \dots, n_{d,p},$$

for some parameters $\{k_\ell\} \subset \mathbb{R}$ and directions $\{\mathbf{d}_\ell\} \subset \mathcal{S}_1^d := \{\mathbf{v} \in \mathbb{R}^d, |\mathbf{d}| = 1\}$, which can be chosen differently in each cell K . It is immediate to verify that $i \frac{\partial \phi_\ell}{\partial t} + \Delta \phi_\ell - V \phi_\ell = 0$ in K . These exponential solutions are called ‘‘pseudoplane waves’’ in the context of Fresnel optics in [12, eq. (11)].

In the following we choose the local dimension $n_{d,p}$ in dependence of the dimension d of the problem and a ‘‘degree’’ parameter p . The parameter p is to be understood as the degree of the polynomial space $\mathbb{P}^p(K)$ providing the same h -convergence rates of $\mathbb{T}_p(K)$. The Trefftz property allows to construct $\mathbb{T}_p(K)$ with dimension $n_{d,p} \ll \dim(\mathbb{P}^p(K))$.

The approximation theory in subsection 4.2 is not restricted to the complex-exponential basis functions in (4.1), in fact it allows any Trefftz basis satisfying Condition 4.4. This condition requires that the discrete space can ‘‘replicate’’ the Taylor polynomial of degree p of any Schrödinger solution. We expect that the same condition can be shown for other Trefftz bases that can be computationally convenient for some geometries Ω or potentials V . For instance, in two space dimensions, in the presence of circular symmetries, one could define a discrete Trefftz space with basis $b_{\ell,m}(r, \theta, t) = J_\ell(k_m r) e^{i\ell\theta} e^{-ik_m^2 t}$ for a set of $\ell \in \mathbb{Z}$ and $k_m \in \mathbb{R}$, where $J_\ell(\cdot)$ is the ℓ th first-order Bessel function and (r, θ) are the polar coordinates in the plane.

4.1. Notation and preliminary results. We use the standard multi-index notation for partial derivatives and monomials, adapted to the space-time setting: for $\mathbf{j} = (\mathbf{j}_\mathbf{x}, j_t) = (j_{x_1}, \dots, j_{x_d}, j_t) \in \mathbb{N}_0^{d+1}$,

$$\begin{aligned} \mathbf{j}! &:= j_{x_1}! \cdots j_{x_d}! j_t!, & |\mathbf{j}| &:= |\mathbf{j}_\mathbf{x}| + j_t := j_{x_1} + \cdots + j_{x_d} + j_t, \\ D^{\mathbf{j}} f &:= \partial_{x_1}^{j_{x_1}} \cdots \partial_{x_d}^{j_{x_d}} \partial_t^{j_t} f, & \mathbf{x}^{\mathbf{j}} t^{j_t} &:= x_1^{j_{x_1}} \cdots x_d^{j_{x_d}} t^{j_t}. \end{aligned}$$

DEFINITION 4.1 (Taylor polynomial). *On an open and bounded set $D \subset \mathbb{R}^{d+1}$, the Taylor polynomial of order $m \in \mathbb{N}$ (and degree $m - 1$), centered at $(\mathbf{z}, s) \in D$, of a function $\varphi \in \mathcal{C}^{m-1}(D)$ is denoted*

$$T_{(\mathbf{z}, s)}^m[\varphi](\mathbf{x}, t) := \sum_{|\mathbf{j}| < m} \frac{1}{\mathbf{j}!} D^{\mathbf{j}} \varphi(\mathbf{z}, s) (\mathbf{x} - \mathbf{z})^{\mathbf{j}_\mathbf{x}} (t - s)^{j_t}.$$

If $\varphi \in \mathcal{C}^m(D)$ and the segment $[(\mathbf{z}, s), (\mathbf{x}, t)] \subset D$, the Lagrange’s form of the Taylor remainder (see [6], Corollary 3.19) is bounded as follows:

$$\begin{aligned} \left| \varphi(\mathbf{x}, t) - T_{(\mathbf{z}, s)}^m[\varphi](\mathbf{x}, t) \right| &\leq |\varphi|_{\mathcal{C}^m(K)} \sum_{|\mathbf{j}|=m} \frac{1}{\mathbf{j}!} (\mathbf{x} - \mathbf{z})^{\mathbf{j}_\mathbf{x}} (t - s)^{j_t} \\ (4.2) \qquad \qquad \qquad &\leq \frac{(d+1)^{m/2}}{m!} h_D^m |\varphi|_{\mathcal{C}^m(D)}, \end{aligned}$$

where h_D is the diameter of D , and we used the multinomial theorem $((\sum_{r=1}^{d+1} v_r)^m = \sum_{|\mathbf{j}|=m} \frac{m!}{\mathbf{j}!} \mathbf{v}^{\mathbf{j}}$) and $|\mathbf{v}|_1 \leq (d+1)^{1/2} |\mathbf{v}|_2 \quad \forall \mathbf{v} \in \mathbb{C}^{d+1}$.

In order to prove approximation results for solutions belonging to spaces more general than $\mathcal{C}^m(Q)$, we introduce the averaged Taylor polynomial as presented in [8] (see also a refined version in [5, Def. 4.1.3]).

DEFINITION 4.2 (Averaged Taylor polynomial). *Let $D \subset \mathbb{R}^{d+1}$, $1 \leq d \in \mathbb{N}$, be an open and bounded set, with diameter h_D , star-shaped with respect to the ball*

$B := B_{\rho h_D}(\mathbf{z}, s)$ centered at $(\mathbf{z}, s) \in D$ and with radius ρh_D , for some $0 < \rho \leq \frac{1}{2}$. If $\varphi \in H^{m-1}(D)$, the averaged Taylor polynomial of order m (and degree $m-1$) is defined as

$$(4.3) \quad \mathcal{Q}^m[\varphi](\mathbf{x}, t) := \frac{1}{|B|} \int_B T_{(\mathbf{z}, s)}^m[\varphi](\mathbf{x}, t) dV(\mathbf{z}, s).$$

We recall the result of [5, Prop. (4.1.17)]:

$$(4.4) \quad D^j T_{(\mathbf{z}, s)}^m[\varphi] = T_{(\mathbf{z}, s)}^{m-|j|}[D^j \varphi], \quad D^j \mathcal{Q}^m[\varphi] = \mathcal{Q}^{m-|j|}[D^j \varphi], \quad |\mathbf{j}| < m.$$

The following Bramble–Hilbert lemma provides an estimate for the error of the averaged Taylor polynomial, see [8] and [5, Thm. 4.3.8].

LEMMA 4.3 (Bramble–Hilbert). *Under the conditions in Definition 4.2, if $\varphi \in H^m(D)$, then*

$$(4.5) \quad \|D^j(\varphi - \mathcal{Q}^m[\varphi])\|_{L^2(D)} \leq C_{d,m,\rho} h_D^{m-|\mathbf{j}|} |\varphi|_{H^m(D)}, \quad \text{for } |\mathbf{j}| \leq m.$$

The explicit value of $C_{d,m,\rho} > 0$ is stated in [8, p. 986] in dependence of d , m and ρ , with the last of these parameters as in Definition 4.2. The last key ingredient is the trace inequality, [5, Theorem 1.6.6], which can be written for any element $K = K_{\mathbf{x}} \times I_n \in \mathcal{T}_h(Q)$ in our space–time setting as

$$(4.6) \quad \begin{aligned} \|\varphi\|_{L^2(K_{\mathbf{x}} \times \{t_{n-1}, t_n\})}^2 &\leq C_{\text{tr}} \left(h_n^{-1} \|\varphi\|_{L^2(K)}^2 + h_n \|\partial_t \varphi\|_{L^2(K)}^2 \right), \quad \forall \varphi \in H^1(I_n; L^2(K_{\mathbf{x}})), \\ \|\varphi\|_{L^2(\partial K_{\mathbf{x}} \times I_n)}^2 &\leq C_{\text{tr}} \left(h_{K_{\mathbf{x}}}^{-1} \|\varphi\|_{L^2(K)}^2 + h_{K_{\mathbf{x}}} \|\nabla \varphi\|_{L^2(K)^d}^2 \right), \quad \forall \varphi \in L^2(I_n; H^1(K_{\mathbf{x}})), \end{aligned}$$

where C_{tr} only depends on the shape-regularity parameter $\text{sr}(\mathcal{T}_h)$ of the space mesh.

4.2. General approximation estimate. We now give a condition on the discrete Trefftz space $\mathbb{T}_p(K)$ and show how it entails h -approximation estimates. In the next sections we describe concrete spaces that satisfy this condition.

Condition 4.4 states that for any sufficiently smooth Schrödinger solution ψ , the discrete Trefftz space contains an element whose Taylor polynomial matches that of ψ . We also require that the coefficients of this approximant are bounded in a suitable sense, so this is a condition on the basis rather than on the discrete space itself. To allow general $\psi \in H^{p+1}(K)$, whose Taylor polynomial might not be defined everywhere and does not guarantee enough approximation, we match $T_{(\mathbf{z}, s)}^{p+1}[\psi]$ in almost every point in a ball B (see Remarks 4.5 and 4.7).

CONDITION 4.4. *Let $B \subset K$ be a $(d+1)$ -dimensional ball such that K is star-shaped with respect to B . Let $\{\phi_1, \dots, \phi_{n_{d,p}}\} \subset C^\infty(K)$ be a basis of $\mathbb{T}^p(K)$. For every $\psi \in \mathbf{T}(K) \cap H^{p+1}(K)$, there exists a vector-valued function $\mathbf{a} \in L^1(B)^{n_{d,p}}$ satisfying the following two conditions*

$$(4.7a) \quad D^j \psi(\mathbf{z}, s) = \sum_{\ell=1}^{n_{d,p}} a_\ell(\mathbf{z}, s) D^j \phi_\ell(\mathbf{z}, s) \quad \text{for all } |\mathbf{j}| \leq p \quad \text{and a.e. } (\mathbf{z}, s) \in B,$$

$$(4.7b) \quad \|\mathbf{a}\|_{L^1(B)} = \int_B \sum_{\ell=1}^{n_{d,p}} |a_\ell(\mathbf{z}, s)| dV(\mathbf{z}, s) \leq C_* |K|^{1/2} \|\psi\|_{H^{p+1}(K)},$$

where $C_* > 0$ might depend on $d, p, \{\phi_\ell\}$ but is independent of K and ψ .

Multiplying (4.7a) with $\frac{(\mathbf{x}-\mathbf{z})^{j\mathbf{x}}(t-s)^{j\mathbf{t}}}{j!}$ and summing over \mathbf{j} , we observe that [Condition 4.4](#) implies that for every smooth Schrödinger solution ψ there is an element of the discrete space $\mathbb{T}_p(K)$ whose Taylor polynomial at (\mathbf{z}, s) coincides with that of ψ :

$$(4.8) \quad T_{(\mathbf{z},s)}^{p+1}[\psi](\mathbf{x},t) = T_{(\mathbf{z},s)}^{p+1}\left[\sum_{\ell=1}^{n_{d,p}} a_\ell(\mathbf{z},s)\phi_\ell\right](\mathbf{x},t) = \sum_{\ell=1}^{n_{d,p}} a_\ell(\mathbf{z},s)T_{(\mathbf{z},s)}^{p+1}[\phi_\ell](\mathbf{x},t)$$

for a.e. $(\mathbf{z},s) \in B, \quad \forall(\mathbf{x},t) \in K.$

Remark 4.5. [Condition 4.4](#) requires the point value of the partial derivatives of a Sobolev function in almost every point of B . This is to be understood as follows.

Let $\psi \in H^{p+1}(K)$. By Calderón’s extension theorem [21, Thm. A.4], ψ can be extended to a $\tilde{\psi} \in H^{p+1}(\mathbb{R}^{d+1})$. Then [1, Thm. 10.1.4] implies that there exists a zero-measure set $\Upsilon \subset \mathbb{R}^{d+1}$ such that $\tilde{\psi}$ admits a “differential of order p ” at every point (\mathbf{z}, s) of the complement of Υ . The differential of order p , as defined in [1, Def. 10.1.3], is a polynomial that coincides with the Taylor polynomial $T_{(\mathbf{z},s)}^{p+1}[\tilde{\psi}]$ whenever this is defined. With a small abuse of notation, this is the polynomial appearing at the left-hand side of (4.8) for all $(\mathbf{z}, s) \in B \setminus \Upsilon$ (while $\phi_\ell \in C^\infty(K)$ so their Taylor polynomials are the classical ones). The partial derivatives $D^{\mathbf{j}}\psi(\mathbf{z}, s)$ in (4.7a) are the partial derivatives of $T_{(\mathbf{z},s)}^{p+1}[\psi]$ evaluated in (\mathbf{z}, s) .

PROPOSITION 4.6. *Let $K \in \mathcal{T}_h(Q)$ and $\psi \in \mathbf{T}(K) \cap H^{p+1}(K)$, with K satisfying the conditions in [Definition 4.2](#). Assume that $\mathbb{T}_p(K)$ satisfies [Condition 4.4](#). Then, there exists an element $\Phi \in \mathbb{T}_p(K)$ and $C > 0$ independent of h_K and ψ such that:*

$$(4.9) \quad \|D^{\mathbf{j}}(\psi - \Phi)\|_{L^2(K)} \leq Ch_K^{p+1-|\mathbf{j}|} \|\psi\|_{H^{p+1}(K)}, \quad 0 \leq |\mathbf{j}| \leq p.$$

Proof. Let $\mathbf{a} \in L^1(B)$ be the coefficient function defined by [Condition 4.4](#). We define the discrete Trefftz function $\Phi \in \mathbb{T}_p(K)$ as

$$(4.10) \quad \begin{aligned} \Phi(\mathbf{x},t) &:= \frac{1}{|B|} \int_B \sum_{\ell=1}^{n_{d,p}} a_\ell(\mathbf{z},s)\phi_\ell(\mathbf{x},t) dV(\mathbf{z},s) \\ &= \frac{1}{|B|} \sum_{\ell=1}^{n_{d,p}} \left(\int_B a_\ell(\mathbf{z},s) dV(\mathbf{z},s) \right) \phi_\ell(\mathbf{x},t). \end{aligned}$$

Since $\Phi \in C^\infty(\overline{K})$, by the triangle inequality, for $|\mathbf{j}| \leq p$ we have

$$(4.11) \quad \|D^{\mathbf{j}}(\psi - \Phi)\|_{L^2(K)} \leq \|D^{\mathbf{j}}(\psi - \mathcal{Q}^{p+1}[\psi])\|_{L^2(K)} + \|D^{\mathbf{j}}(\mathcal{Q}^{p+1}[\psi] - \Phi)\|_{L^2(K)}.$$

The first term is bounded by the Bramble–Hilbert [Lemma 4.3](#), while for the second term we first derive a pointwise estimate for all $(\mathbf{x}, t) \in K$ and $|\mathbf{j}| \leq p$ using the multivariate Taylor’s theorem and the fact that $\phi_\ell \in C^\infty(K)$:

$$\begin{aligned} &|D^{\mathbf{j}}(\mathcal{Q}^{p+1}[\psi](\mathbf{x},t) - \Phi(\mathbf{x},t))| \\ &\stackrel{(4.3),(4.10)}{=} \left| \frac{1}{|B|} \int_B D^{\mathbf{j}} \left(T_{(\mathbf{z},s)}^{p+1}[\psi](\mathbf{x},t) - \sum_{\ell=1}^{n_{d,p}} a_\ell(\mathbf{z},s)\phi_\ell(\mathbf{x},t) \right) dV(\mathbf{z},s) \right| \\ &\stackrel{(4.8)}{=} \left| \frac{1}{|B|} \int_B \sum_{\ell=1}^{n_{d,p}} a_\ell(\mathbf{z},s) D^{\mathbf{j}} \left(T_{(\mathbf{z},s)}^{p+1}[\phi_\ell](\mathbf{x},t) - \phi_\ell(\mathbf{x},t) \right) dV(\mathbf{z},s) \right| \end{aligned}$$

$$\begin{aligned}
&\stackrel{(4.4)}{=} \left| \frac{1}{|B|} \int_B \sum_{\ell=1}^{n_{d,p}} a_\ell(\mathbf{z}, s) \left(T_{(\mathbf{z},s)}^{p+1-|\mathbf{j}|} [D^{\mathbf{j}} \phi_\ell](\mathbf{x}, t) - D^{\mathbf{j}} \phi_\ell(\mathbf{x}, t) \right) dV(\mathbf{z}, s) \right| \\
&\stackrel{(4.2)}{\leq} \frac{(d+1)^{(p+1-|\mathbf{j}|)/2}}{|B|(p+1-|\mathbf{j}|)!} h_K^{p+1-|\mathbf{j}|} \max_{\ell=1, \dots, n_{d,p}} \left\{ |\phi_\ell|_{C^{p+1}(K)} \right\} \int_B |\mathbf{a}(\mathbf{z}, s)|_1 dV(\mathbf{z}, s) \\
&\stackrel{(4.7b)}{\leq} \frac{|K|^{1/2} (d+1)^{(p+1-|\mathbf{j}|)/2}}{|B|(p+1-|\mathbf{j}|)!} h_K^{p+1-|\mathbf{j}|} \max_{\ell=1, \dots, n_{d,p}} \left\{ |\phi_\ell|_{C^{p+1}(K)} \right\} C_\star \|\psi\|_{H^{p+1}(K)}.
\end{aligned}$$

Then

$$\begin{aligned}
&\|D^{\mathbf{j}}(\mathcal{Q}^{p+1}[\psi] - \Phi)\|_{L^2(K)} \\
&\leq \frac{|K|}{|B|} \frac{(d+1)^{(p+1-|\mathbf{j}|)/2}}{(p+1-|\mathbf{j}|)!} h_K^{p+1-|\mathbf{j}|} \max_{\ell=1, \dots, n_{d,p}} \left\{ |\phi_\ell|_{C^{p+1}(K)} \right\} C_\star \|\psi\|_{H^{p+1}(K)},
\end{aligned}$$

which, combined with $|K| \leq |B_{h_K}| \leq \rho^{d+1} |B_{\rho h_K}| = \rho^{d+1} |B|$, the triangle inequality (4.11) and Bramble–Hilbert lemma estimate (4.5), completes the proof. \square

No special property of the Schrödinger equation has been used in the proof of [Proposition 4.6](#): the same result extends to any linear PDE for which one has at hand a discrete Trefftz space that can reproduce the Taylor polynomials of any PDE solution.

Remark 4.7. The use of averaged Taylor polynomials $\mathcal{Q}^m[\cdot]$ (4.3) allows to treat any $\psi \in H^{p+1}(K)$. Under the stronger assumption $\psi \in C^{p+1}(K)$ the argument of [Proposition 4.6](#) simplifies considerably: one could use the standard Taylor polynomial $T_{(\mathbf{z},s)}^m[\cdot]$, assume that K is star-shaped with respect to a point, and require the identity (4.7a) for a single point (\mathbf{z}, s) only.

4.3. Best approximation in the (1+1)-dimensional case. The next proposition shows that, in one space dimension, the choice of exponential basis functions (4.1) with different values of k_ℓ (and equal direction $d_\ell = 1$) is enough to ensure [Condition 4.4](#) and the approximation properties of $\mathbb{T}^p(K)$. Only $2p+1$ degrees of freedom per element are needed to obtain h^p convergence. An example of the basis (4.12) for $p=3$ is plotted in [Figure 1](#).

PROPOSITION 4.8. *Let $d=1$, $p \in \mathbb{N}$, $n_{1,p} = 2p+1$ and the parameters $\{k_\ell\}_{\ell=1}^{2p+1} \subset \mathbb{R}$ be all different from one another. Let*

$$(4.12) \quad \phi_\ell(x, t) = \exp \left[i(k_\ell x - (k_\ell^2 + V|_K)t) \right], \quad \ell = 1, \dots, 2p+1,$$

be the basis of the discrete Trefftz space $\mathbb{T}^p(K)$. Then [Condition 4.4](#) is satisfied.

Proof. Let $\psi \in \mathbf{T}(K) \cap H^{p+1}(K)$ and let Υ be the zero-measure set introduced in [Remark 4.5](#). Let $(z, s) \in B \setminus \Upsilon$. Since all the derivatives of ψ of order at most p are defined at (z, s) and each basis function $\phi_\ell \in C^\infty(K)$, the Taylor polynomials centered at (z, s) of order $p+1$ of ψ and each ϕ_ℓ can be written as:

$$(4.13a) \quad T_{(z,s)}^{p+1}[\psi](x, t) = \sum_{j_x=0}^p \sum_{j_t=0}^{p-j_x} b_{\mathbf{j}}(x-z)^{j_x} (t-s)^{j_t}, \quad \text{where } \mathbf{j} = (j_x, j_t),$$

$$(4.13b) \quad T_{(z,s)}^{p+1}[\phi_\ell](x, t) = \sum_{j_x=0}^p \sum_{j_t=0}^{p-j_x} M_{\mathbf{j}, \ell} (x-z)^{j_x} (t-s)^{j_t} \quad \text{for } \ell = 1, \dots, n_{1,p}.$$

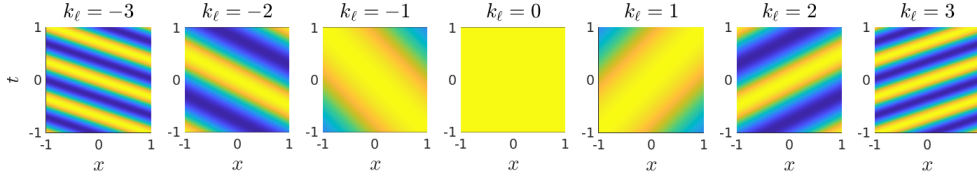


Fig. 1: The real parts ($\cos(k_\ell x - k_\ell^2 t)$) of the Trefftz basis functions ϕ_ℓ of (4.12) for the potential $V = 0$ and $p = 3$, plotted on the space-time square $(x, t) \in (-1, 1) \times (-1, 1)$. The parameters k_ℓ are chosen as $k_\ell = -3, -2, \dots, 3$. These functions can be thought as plane waves $\phi_\ell(x, t) = e^{i\kappa(v_x, v_t)^\top(x, t)}$ in the xt plane with different wavenumbers $\kappa = \sqrt{k_\ell^2 + k_\ell^4}$ and directions $(v_x, v_t) = (k_\ell, -k_\ell^2)/\sqrt{k_\ell^2 + k_\ell^4}$. The space- and time-frequencies increase linearly and quadratically with $|k_\ell|$, respectively. The space spanned by these $n_{1,3} = 7$ basis functions approximates Schrödinger solutions with the same convergence rates of cubic polynomials.

We aim to prove that there exists $\mathbf{a}(z, s) \in \mathbb{C}^{2p+1}$ that satisfies (4.7a), i.e.,

$$\sum_{\ell=1}^{n_{1,p}} a_\ell(z, s) M_{\mathbf{j}, \ell} = b_{\mathbf{j}}, \quad \text{for } |\mathbf{j}| \leq p, \quad \mathbf{j} = (j_x, j_t).$$

This can be arranged as a rectangular linear system of the form $\mathbf{M} \mathbf{a}(z, s) = \mathbf{b}$, with $\mathbf{b} \in \mathbb{C}^{r_p}$ and $\mathbf{M} \in \mathbb{C}^{r_p \times n_{1,p}}$, $r_p = (p+1)(p+2)/2$.

The case $p = 1$ is rather special, since $n_{1,1} = r_1 = 3$ and the matrix \mathbf{M} is square; hence we just need to show that it is not singular. For $p \geq 2$ we need, in addition, to construct a subset $\mathcal{D} \subset \mathbb{C}^{r_p}$ containing both $\text{Im}(\mathbf{M})$ and \mathbf{b} . We first note that for all smooth $\varphi \in \mathbf{T}(K)$ and each multi-index \mathbf{j} , with $|\mathbf{j}| \leq p$, $D^{\mathbf{j}} \varphi(z, s) = D^{\mathbf{j}} T_{(z,s)}^{p+1}[\varphi](z, s)$. Since φ and its derivatives satisfy the Schrödinger equation, this implies that $D^{\mathbf{j}} T_{(z,s)}^{p+1}[\varphi]$ satisfies the same equation at the single point (z, s) :

$$(4.14) \quad \left(\left(i \frac{\partial}{\partial t} + \Delta - V \right) D^{\mathbf{j}} T_{(z,s)}^{p+1}[\varphi] \right) (z, s) = 0, \quad \text{for } p \geq 2 \text{ and } |\mathbf{j}| \leq p-2.$$

We want to express these equations in terms of the coefficients of $T_{(z,s)}^{p+1}[\varphi](x, t)$. Setting $\mathbf{C} \in \mathbb{C}^{r_p}$ to be the vector with components $C_{j_x j_t} := \frac{1}{\mathbf{j}!} D^{\mathbf{j}} \varphi(z, s)$, so that $T_{z,s}^{p+1}[\varphi](x, t) = \sum_{|\mathbf{j}| \leq p} C_{j_x j_t} (x-z)^{j_x} (t-s)^{j_t}$, we have

$$\begin{aligned} \frac{\partial}{\partial t} T_{z,s}^{p+1}[\varphi](x, t) &= \sum_{j_x=0}^p \sum_{j_t=0}^{p-1-j_x} C_{j_x(j_t+1)} (j_t+1) (x-z)^{j_x} (t-s)^{j_t}, \\ \frac{\partial^2}{\partial x^2} T_{z,s}^{p+1}[\varphi](x, t) &= \sum_{j_x=0}^{p-2} \sum_{j_t=0}^{p-2-j_x} C_{(j_x+2)j_t} (j_x+1)(j_x+2) (x-z)^{j_x} (t-s)^{j_t}. \end{aligned}$$

Expanding (4.14), we get the following $p(p-1)/2$ relations between the coefficients of the Taylor polynomial of φ :

$$(4.15) \quad i(j_t+1)C_{j_x(j_t+1)} + (j_x+1)(j_x+2)C_{(j_x+2)j_t} = VC_{j_x, j_t}, \\ \text{for } |\mathbf{j}| \leq p-2, \quad \mathbf{j} = (j_x, j_t).$$

We define $\mathcal{D} := \{\mathbf{C} \in \mathbb{C}^{r_p} \mid \mathbf{C} \text{ satisfies (4.15)}\}$: since $\psi, \phi_\ell \in \mathbf{T}(K)$, it is evident that $\mathbf{b} \in \mathcal{D}$ and $\text{Im}(\mathbf{M}) \subset \mathcal{D}$.

The key point of the proof is to show that $\text{rank}(\mathbf{M}) = \dim(\mathcal{D}) = 2p + 1$, which guarantees that the overdetermined linear system $\mathbf{M}\mathbf{a}(z, s) = \mathbf{b}$ has a unique solution.

Figure 2 illustrates the relations that define \mathcal{D} for both cases $V = 0$ and $V \neq 0$. It shows that given the $2p + 1$ entries $C_{j_x j_t}$ of $\mathbf{C} \in \mathcal{D}$ corresponding to $j_x \in \{0, 1\}$, all other entries are uniquely determined by the conditions (4.15). Therefore

$$\text{rank}(\mathbf{M}) \leq \dim(\mathcal{D}) \leq 2p + 1.$$

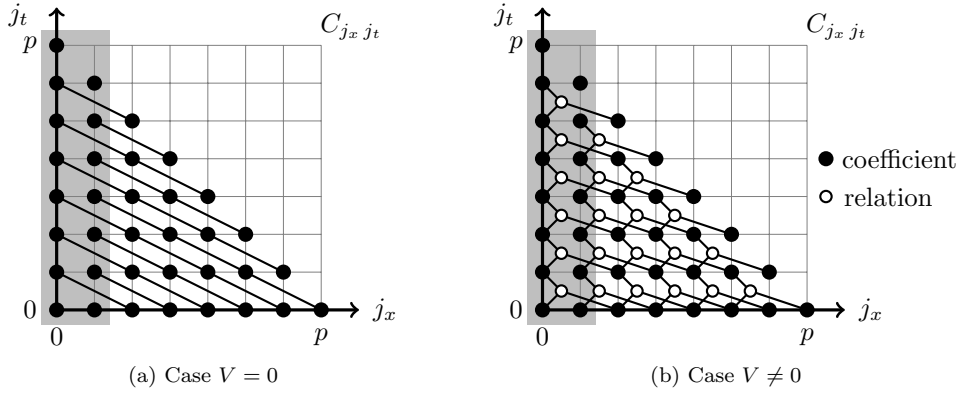


Fig. 2: Illustration of the relations defining the set \mathcal{D} in the (1+1)-dimensional case. The black dots in the (j_x, j_t) plane represent the coefficients $C_{j_x j_t}$ of $\mathbf{C} \in \mathcal{D} \subset \mathbb{C}^{r_p}$, $r_p = \frac{(p+1)(p+2)}{2}$. In the case $V \neq 0$ (right panel), each shape connects three black dots located at the points $(j_x, j_t + 1)$, (j_x, j_t) and $(j_x + 2, j_t)$: this shape represents one of the equations (4.15) which, given $C_{j_x(j_t+1)}$ and $C_{j_x j_t}$, allows to compute $C_{(j_x+2)j_t}$. If the $2p + 1$ values with $j_x \in \{0, 1\}$ (corresponding to the nodes in the shaded region) are given, then these relations uniquely determine all the other coefficients, which can be computed sequentially by proceeding left to right in the diagram. In the figure $p = 7$, the number of nodes is $r_p = 36$, the number of nodes in the shaded region is $n_{1,p} = 15$, the number of relations is $r_p - n_{1,p} = 21$. The case $V = 0$ (left panel) is slightly simpler: the coefficient $C_{(j_x+2)j_t}$ is determined by $C_{j_x(j_t+1)}$ only and each relation in (4.15) is depicted as a segment .

The rest of the proof consists in proving that $\text{rank}(\mathbf{M}) \geq 2p + 1$. To do so, we first recall that $\phi_\ell(x, t) = \exp[i(k_\ell x - (k_\ell^2 + V)t)]$ from the basis definition (4.1), and observe that the entries of matrix \mathbf{M} are given by

$$M_{\mathbf{j}, \ell} = \frac{1}{j_x! j_t!} D^{\mathbf{j}} \phi_\ell(z, s) = q_{j_x, j_t}(k_\ell) \phi_\ell(z, s), \quad \mathbf{j} = (j_x, j_t), \quad \ell = 1, \dots, 2p + 1,$$

where $q_{j_x, j_t}(k) = \frac{1}{j_x! j_t!} (ik)^{j_x} (-i(k^2 + V))^{j_t}$ is a complex-valued polynomial of degree exactly $j_x + 2j_t$. We define a square submatrix \mathbf{M}_\square of the matrix \mathbf{M} by taking the rows corresponding to $j_x \in \{0, 1\}$. This, in turn, can be decomposed as $\mathbf{M}_\square = \mathbf{V} \mathbf{D}_{z, s}$, where $\mathbf{D}_{z, s} = \text{diag}(\phi_1(z, s), \dots, \phi_{2p+1}(z, s))$ and the Vandermonde-like matrix $\mathbf{V} \in$

$\mathbb{C}^{(2p+1) \times (2p+1)}$ is given by

$$(4.16) \quad \mathbf{V} = \begin{pmatrix} q_{0,0}(k_1) & q_{0,0}(k_2) & \cdots & q_{0,0}(k_{2p+1}) \\ q_{1,0}(k_1) & q_{1,0}(k_2) & \cdots & q_{1,0}(k_{2p+1}) \\ \vdots & \vdots & & \vdots \\ q_{0,j_t}(k_1) & q_{0,j_t}(k_2) & \cdots & q_{0,j_t}(k_{2p+1}) \\ q_{1,j_t}(k_1) & q_{1,j_t}(k_2) & \cdots & q_{1,j_t}(k_{2p+1}) \\ \vdots & \vdots & & \vdots \\ q_{0,p-1}(k_1) & q_{0,p-1}(k_2) & \cdots & q_{0,p-1}(k_{2p+1}) \\ q_{1,p-1}(k_1) & q_{1,p-1}(k_2) & \cdots & q_{1,p-1}(k_{2p+1}) \\ q_{0,p}(k_1) & q_{0,p}(k_2) & \cdots & q_{0,p}(k_{2p+1}) \end{pmatrix}.$$

We observe that $V_{m,\ell} = p_{m-1}(k_\ell)$, $m = 1, \dots, 2p+1$, for some polynomials $p_m(\cdot)$ of degree m . Therefore there exists a lower triangular matrix \mathbf{P} such that $\mathbf{P}\mathbf{V} = \tilde{\mathbf{V}}$, where $\tilde{V}_{m,\ell} = k_\ell^{m-1}$ for $m, \ell = 1, \dots, 2p+1$. (The entries of the m th row of the inverse of \mathbf{P} are the coefficients of the monomial expansion of the polynomial p_{m-1} .) This means that $\tilde{\mathbf{V}}$ is a Vandermonde matrix, so it is invertible [13, §22.1] (recall that all k_ℓ are different from one another). We conclude that the matrix \mathbf{V} is invertible, independent of (z, s) and \mathbf{M} is full rank (namely, $\text{rank}(\mathbf{M}) = 2p+1$).

Denoting by \mathbf{b}_\square the subvector of \mathbf{b} corresponding to the indices $j_x \in \{0, 1\}$, the unique solution of the linear system $\mathbf{M}\mathbf{a}(z, s) = \mathbf{b}$ is $\mathbf{a}(z, s) = \mathbf{M}_\square^{-1}\mathbf{b}_\square$ and satisfies condition (4.7a). Moreover, the following bound holds

$$(4.17) \quad \|\mathbf{a}(z, s)\|_1 \leq \|\mathbf{V}^{-1}\|_1 \|\mathbf{D}_{z,s}^{-1}\|_1 \|\mathbf{b}_\square\|_1,$$

where $\|\mathbf{D}_{z,s}^{-1}\|_1 = 1$ for all $(z, s) \in B$. We now recall that (z, s) was chosen arbitrarily in $B \setminus \Upsilon$. Setting $\mathbf{a}(z, s) = \mathbf{0}$ and $\mathbf{b}_\square(z, s) = \mathbf{0}$ for $(z, s) \in \Upsilon$ (which has zero measure), recalling from (4.13a) that $b_j = \frac{1}{j!} D^j \psi$, and integrating (4.17) over B , we obtain

$$\begin{aligned} \|\mathbf{a}\|_1 \|L^1(B)\| &\leq \|\mathbf{V}^{-1}\|_1 \|\mathbf{b}_\square\|_1 \|L^1(B)\| \leq \|\mathbf{V}^{-1}\|_1 \sqrt{2p+1} \|\mathbf{b}_\square\|_2 \|L^1(B)\| \\ &\leq \|\mathbf{V}^{-1}\|_1 \sqrt{2p+1} \sqrt{|B|} \|\psi\|_{H^{p+1}(B)}. \end{aligned}$$

This implies the assertion (4.7b) with $C_\star = \|\mathbf{V}^{-1}\|_1 \sqrt{2p+1}$, since $|B| \leq |K|$. \square

4.4. Best approximation in the (2+1)-dimensional case. Following the same strategy of the previous section, in Proposition 4.9 we show that, for a sensible choice of the parameters $\{k_\ell\}$ and the directions $\{\mathbf{d}_\ell\}$ in (4.1), Condition 4.4 is true for $\mathbb{T}_p(\mathcal{T}_h)$ in the (2+1)-dimensional case.

The basis functions $\phi_{m,\lambda}$ are plane waves in space indexed by two parameters: m identifying the wavenumber k_m , and λ identifying the propagation direction $\theta_{m,\lambda}$. For every wavenumber we take a different number of directions following a strategy similar to that used for the construction of plane-wave Trefftz bases for the 3D Helmholtz equation in [22, Lemma 4.2]. The time-dependence of each basis element is harmonic with frequency $k_m^2 + V|_K$. A sample basis for $p = 2$ is shown in Figure 3.

PROPOSITION 4.9. *Let $d = 2$ and $n_{2,p} = (p+1)^2$. Let the parameters k_m and $\theta_{m,\lambda}$ satisfy the following conditions:*

$$\begin{aligned} k_m &\in \mathbb{R} \text{ for } m = 0, \dots, p, \text{ with } k_{m_1}^2 \neq k_{m_2}^2 \text{ for } m_1 \neq m_2 \text{ and } k_m \neq 0, \\ \theta_{m,\lambda} &\in [0, 2\pi) \text{ for } m = 0, \dots, p, \lambda = 1, \dots, 2m+1, \text{ with } \theta_{m,\lambda_1} \neq \theta_{m,\lambda_2} \text{ for } \lambda_1 \neq \lambda_2. \end{aligned}$$

Define the directions $\mathbf{d}_{m,\lambda} = (\cos \theta_{m,\lambda}, \sin \theta_{m,\lambda})$ and the basis functions

$$\phi_{m,\lambda}(\mathbf{x}, t) = \exp \left[i \left(k_m \mathbf{d}_{m,\lambda}^\top \mathbf{x} - (k_m^2 + V|_K)t \right) \right] \quad \text{for } m = 0, \dots, p, \lambda = 1, \dots, 2m + 1.$$

Then [Condition 4.4](#) holds true.

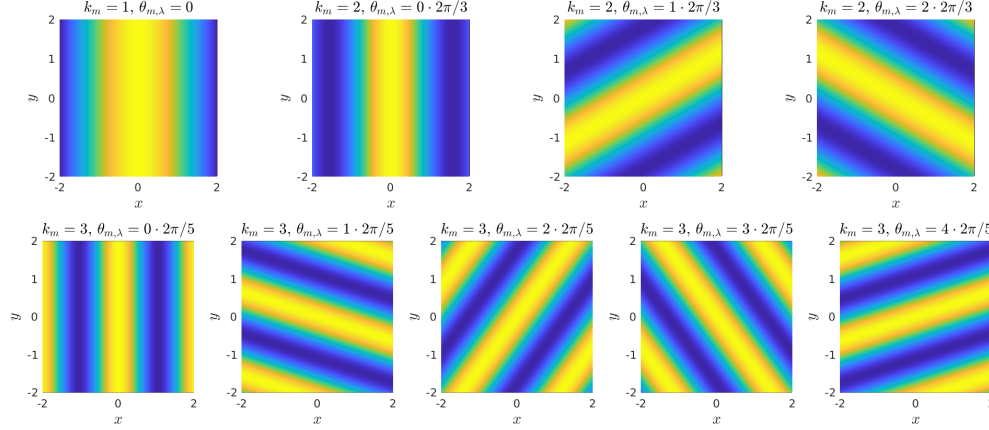


Fig. 3: The real parts of the Trefftz basis functions defined in (4.9) for $V = 0$ and $p = 2$ at time $t = 0$ on the space domain $(-2, 2)^2$. Here $k_m = m + 1$ for $m = 0, 1, 2$ and $\theta_{m,\lambda} = 2\pi \frac{\lambda-1}{2m+1}$ for $\lambda = 1, \dots, 2m + 1$. Note that, differently from Figure 1, here we only plot the space dependence of the ϕ_ℓ .

Proof. Let $\psi \in \mathbf{T}(K) \cap H^{p+1}(K)$ and $(\mathbf{z}, s) \subset B \setminus \Upsilon$, with the set Υ as in [Remark 4.5](#). As in [Proposition 4.8](#) we can arrange the coefficients of the Taylor polynomials of ψ and each basis function ϕ_ℓ in a vector $\mathbf{b} \in \mathbb{C}^{r_p}$ and a matrix $\mathbf{M} \in \mathbb{C}^{r_p \times n_{2,p}}$ with $r_p = (p+1)(p+2)(p+3)/6$. In order to prove (4.7b), we look for a vector $\mathbf{a}(\mathbf{z}, s) \in \mathbb{C}^{n_{2,p}}$ such that $\mathbf{M}\mathbf{a}(\mathbf{z}, s) = \mathbf{b}$.

Similarly to the (1 + 1) dimensional case, $\mathbf{b} \in \mathcal{D}$ and $\text{Im}(\mathbf{M}) \subset \mathcal{D}$ for \mathcal{D} the set of all the vectors $\mathbf{C} \in \mathbb{C}^{r_p}$ satisfying the following relations

$$(4.18) \quad \begin{aligned} i(j_t + 1)C_{j_x j_y (j_t+1)} + (j_x + 1)(j_x + 2)C_{(j_x+2)j_y j_t} \\ + (j_y + 1)(j_y + 2)C_{j_x(j_y+2)j_t} = VC_{j_x j_y j_t} \end{aligned}$$

for $|\mathbf{j}| \leq p - 2$, $\mathbf{j} = (j_x, j_y, j_t)$.

[Figure 4](#) depicts the equations (4.18) as relations between the coefficients of the vector \mathbf{C} , which are represented as points in the (j_x, j_y, j_t) space. In particular, it shows that the $(p+1)^2$ entries of any $\mathbf{C} \in \mathcal{D}$ with $j_x \in \{0, 1\}$ determine all the other entries of \mathbf{C} , thus $\text{rank}(\mathbf{M}) \leq \dim(\mathcal{D}) \leq (p+1)^2$.

Now it just remains to prove that $\text{rank}(\mathbf{M}) \geq (p+1)^2$.

We fix an arbitrary ordering $\ell = 1, \dots, (p+1)^2$ of the “triangular” index set $\{(m, \lambda) : m = 0, \dots, p, \lambda = 1, \dots, 2m + 1\}$, so that we can write ϕ_ℓ , k_ℓ and θ_ℓ for the basis functions $\phi_{m,\lambda}$ and the parameters $k_{m,\lambda}$ and $\theta_{m,\lambda}$.

First, from the basis function definition, the matrix \mathbf{M} can be decomposed as $\mathbf{M} = \mathbf{G}\mathbf{D}_{\mathbf{z},s}$ for the diagonal matrix $\mathbf{D}_{\mathbf{z},s} = \text{diag}(\phi_1(\mathbf{z}, s), \dots, \phi_{(p+1)^2}(\mathbf{z}, s))$ and a matrix $\mathbf{G} \in \mathbb{C}^{r_p \times n_{2,p}}$ with entries independent of (\mathbf{z}, s) given by:

$$(4.19) \quad \mathbf{G}_{\mathbf{j},\ell} = \frac{1}{j_x! j_y! j_t!} (ik_\ell \cos \theta_\ell)^{j_x} (ik_\ell \sin \theta_\ell)^{j_y} (-i(k_\ell^2 + V))^{j_t}, \quad \mathbf{j} = (j_x, j_y, j_t).$$

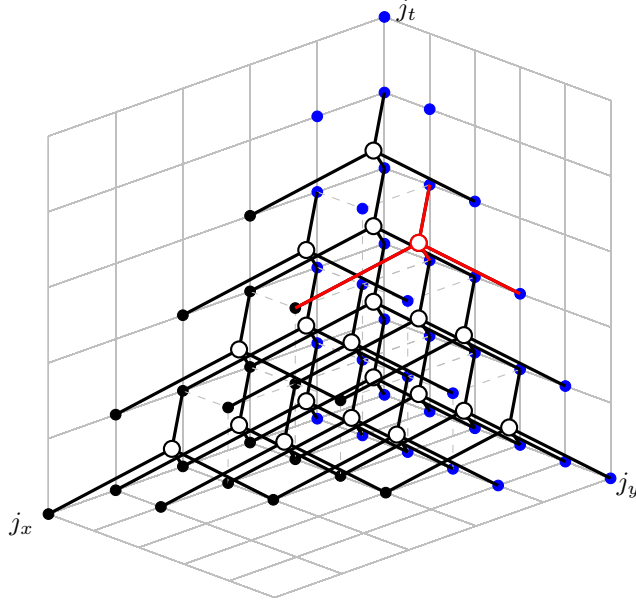


Fig. 4: A representation of the relations defining the set \mathcal{D} in the (2+1)-dimensional case. The colored dots in position $\mathbf{j} = (j_x, j_y, j_t)$, $|\mathbf{j}| \leq p$, correspond to the entries $C_{j_x j_y j_t}$ of the vector $\mathbf{C} \in \mathcal{D} \subset \mathbb{C}^{r_p}$ (here $p = 5$ and $r_p = 56$). Each white circle is connected by the segments to four nodes and represents one of the equations in (4.18): given $C_{j_x j_y j_t}$, $C_{j_x j_y (j_t+1)}$ and $C_{j_x (j_y+2) j_t}$, it allows to compute $C_{(j_x+2) j_y j_t}$ (the leftmost of the four nodes connected to a given white circle). The red dot exemplifies one of these relations, for $\mathbf{j} = (0, 1, 2)$. Given the $(p+1)^2$ coefficients with $j_x \in \{0, 1\}$ (the blue dots), all other coefficients are uniquely determined and $\dim(\mathcal{D}) \leq (p+1)^2$.

We define a square matrix $\mathbf{S} \in \mathbb{C}^{n_{2,p} \times n_{2,p}}$ with the block structure $\mathbf{S} = \begin{pmatrix} \mathbf{S}^+ \\ \mathbf{S}^- \end{pmatrix}$, where $\mathbf{S}^+ \in \mathbb{C}^{\frac{(p+1)(p+2)}{2} \times n_{2,p}}$ and $\mathbf{S}^- \in \mathbb{C}^{\frac{p(p+1)}{2} \times n_{2,p}}$ are defined as

$$S_{(j_x, j_t), \ell}^+ = (k_\ell^2 + V)^{j_t} k_\ell^{j_x} e^{i\theta_\ell j_x} \quad \text{for } \begin{array}{l} j_x = 0, \dots, p, \\ j_t = 0, \dots, p - j_x, \end{array} \quad \ell = 1, \dots, (p+1)^2,$$

$$S_{(j_x, j_t), \ell}^- = (k_\ell^2 + V)^{j_t} k_\ell^{j_x} e^{-i\theta_\ell j_x} \quad \text{for } \begin{array}{l} j_x = 1, \dots, p, \\ j_t = 0, \dots, p - j_x, \end{array} \quad \ell = 1, \dots, (p+1)^2.$$

The binomial theorem allows to relate the blocks \mathbf{S}^\pm to \mathbf{G} :

$$\begin{aligned} S_{(j_x, j_t), \ell}^+ &= (k_\ell^2 + V)^{j_t} (k_\ell \cos \theta_\ell + i k_\ell \sin \theta_\ell)^{j_x} \\ &= \sum_{j_x + j_y = j_x} \frac{j_x!}{j_x! j_y!} (k_\ell \cos \theta_\ell)^{j_x} (i k_\ell \sin \theta_\ell)^{j_y} (k_\ell^2 + V)^{j_t} \\ &= \sum_{j_x + j_y = j_x} \frac{j_t! j_x!}{i^{j_x} (-i)^{j_t}} \mathbf{G}_{\mathbf{j}, \ell}, \end{aligned} \quad \begin{array}{l} j_x = 0, \dots, p, \\ j_t = 0, \dots, p - j_x, \\ \ell = 1, \dots, (p+1)^2, \end{array}$$

$$S_{(j_x, j_t), \ell}^- = (k_\ell^2 + V)^{j_t} (k_\ell \cos \theta_\ell - i k_\ell \sin \theta_\ell)^{j_x}$$

$$\begin{aligned}
&= \sum_{j_x + j_y = j_{\mathbf{x}}} \frac{j_{\mathbf{x}}!}{j_x! j_y!} (k_\ell \cos \theta_\ell)^{j_x} (-i k_\ell \sin \theta_\ell)^{j_y} (k_\ell^2 + V)^{j_t} \\
&= \sum_{j_x + j_y = j_{\mathbf{x}}} \frac{j_t! j_{\mathbf{x}}!}{i^{j_x} (-1)^{j_y} (-i)^{j_t}} \mathbf{G}_{j, \ell}, \quad \begin{array}{l} j_{\mathbf{x}} = 1, \dots, p, \\ j_t = 0, \dots, p - j_{\mathbf{x}}, \\ \ell = 1, \dots, (p+1)^2. \end{array}
\end{aligned}$$

This means that there exists a matrix $\mathbf{P} \in \mathbb{C}^{n_{2,p} \times r_p}$ such that $\mathbf{S} = \mathbf{P}\mathbf{G}$.

Next, we prove that \mathbf{S} is not singular. If $\mathbf{S}^\top \mathbf{c} = \mathbf{0}$ for some vector $\mathbf{c} \in \mathbb{C}^{n_{2,p}}$, then for each pair $(k_m, \theta_{m,\lambda})$ in the definition of the basis functions we have

$$\begin{aligned}
(4.20) \quad 0 &= \sum_{n=-p}^p \left(\sum_{j_t=0}^{p-|n|} c_{n,j_t} (k_m^2 + V)^{j_t} k_m^{|n|} \right) e^{in\theta_{m,\lambda}} = \sum_{n=-p}^p \zeta_n(k_m) e^{in\theta_{m,\lambda}}, \\
& \quad m = 0, \dots, p, \quad \lambda = 1, \dots, 2m+1,
\end{aligned}$$

If we fix $m = p$ in Equation (4.20), the $\zeta_n(k_p)$ are the coefficients of a trigonometric polynomial of degree p with $2p+1$ different zeros $\theta_{p,\lambda}$, which implies that $\zeta_n(k_p) = 0$, for $n = -p, \dots, p$. In particular $0 = \zeta_{\pm p}(k_p) = c_{\pm p,0} k_p^p \Rightarrow c_{\pm p,0} = 0$, since $k_p \neq 0$ by hypothesis.

We now proceed by (backward) induction. Assume that for some $\eta \in \{1, \dots, p\}$ we have:

$$(4.21a) \quad c_{\pm n, j_t} = 0, \quad \text{for } n = p - \eta + 1, \dots, p \text{ and } j_t = 0, \dots, p - |n|,$$

$$(4.21b) \quad \zeta_n(k_m) = 0, \quad \text{for } n = -p, \dots, p \text{ and } m = p - \eta + 1, \dots, p.$$

Then (4.20) gives

$$\sum_{n=-(p-\eta)}^{p-\eta} \zeta_n(k_m) e^{in\theta_{m,\lambda}} = 0,$$

and for $m = (p - \eta)$, the $\zeta_n(k_{p-\eta})$ are the coefficients of a trigonometric polynomial of degree $p - \eta$ with $2(p - \eta) + 1$ different zeros $\theta_{p-\eta,\lambda}$. Therefore assumption (4.21b) also holds for $m = p - \eta$. For $n = \pm(p - \eta)$ in (4.21b) we have

$$k_m^{p-\eta} \sum_{j_t=0}^{\eta} c_{\pm(p-\eta), j_t} (k_m^2 + V)^{j_t} = 0;$$

therefore $c_{\pm(p-\eta), j_t}$ are the coefficients of a complex-valued polynomial of degree η with $\eta + 1$ different zeros $(k_m^2 + V)$, $m = p - \eta, \dots, p$; which implies that assumption (4.21a) holds for $n = p - \eta$. Recursively, this leads to $\mathbf{c} = \mathbf{0}$; therefore the matrix \mathbf{S} is invertible and, since $\mathbf{S} = \mathbf{P}\mathbf{G}$ and $\mathbf{M} = \mathbf{G}\mathbf{D}_{\mathbf{z},s}$ for a nonsingular $\mathbf{D}_{\mathbf{z},s}$, the matrix \mathbf{M} has rank at least $n_{2,p}$ so it is full rank.

The solution $\mathbf{a}(\mathbf{z}, s)$ of the rectangular linear system $\mathbf{M}\mathbf{a}(\mathbf{z}, s) = \mathbf{b}$ is $\mathbf{a}(\mathbf{z}, s) = \mathbf{D}_{\mathbf{z},s}^{-1} \mathbf{S}^{-1} \mathbf{P}\mathbf{b}$, satisfies (4.7a), and the following bound is obtained

$$\|\mathbf{a}(z, s)\|_1 \leq \|\mathbf{S}^{-1}\|_1 \|\mathbf{D}_{\mathbf{z},s}^{-1}\|_1 \|\mathbf{P}\mathbf{b}\|_1,$$

where $\|\mathbf{D}_{\mathbf{z},s}^{-1}\|_1 = 1$ for all $(\mathbf{z}, s) \in B$. Writing $b_j = \frac{1}{j!} D^j \psi(\mathbf{z}, s)$ and integrating over B as in the proof of Proposition 4.8, we obtain (4.7b) with $C_\star = \|\mathbf{S}^{-1}\|_1 \|\mathbf{P}\|_1 \sqrt{r_p}$. \square

4.5. Error bounds in DG norm. The next proposition provides a bound on the $||| \cdot |||_{\text{DG}^+}$ norm in terms of volume Sobolev seminorms and norms and is a direct consequence of the trace inequalities (4.6).

PROPOSITION 4.10. For all $\varphi \in \prod_{K \in \mathcal{T}_h(Q)} H^1(I_n; L^2(K_{\mathbf{x}})) \cap L^2(I_n; H^2(K_{\mathbf{x}}))$, the following bound holds

$$\begin{aligned} |||\varphi|||_{\text{DG}^+}^2 &\leq 3 C_{\text{tr}} \sum_{K \in \mathcal{T}_h(Q)} \left[h_n^{-1} \|\varphi\|_{L^2(K)}^2 + h_n \|\partial_t \varphi\|_{L^2(K)}^2 \right. \\ &\quad + a_K^2 h_{K_{\mathbf{x}}}^{-1} \|\varphi\|_{L^2(K)}^2 + a_K^2 h_{K_{\mathbf{x}}} \|\nabla \varphi\|_{L^2(K)^d}^2 \\ &\quad \left. + b_K^2 h_{K_{\mathbf{x}}}^{-1} \|\nabla \varphi\|_{L^2(K)^d}^2 + b_K^2 h_{K_{\mathbf{x}}} \|D^2 \varphi\|_{L^2(K)^{d \times d}}^2 \right], \end{aligned}$$

where $D^2(\varphi)$ is the space-time Hessian of φ and

$$\begin{aligned} \alpha_{\text{inf}}^K &:= \text{ess inf}_{\partial K \cap (\mathcal{F}_h^{\text{time}} \cup \mathcal{F}_h^{\text{D}})} \alpha, & \beta_{\text{inf}}^K &:= \text{ess inf}_{\partial K \cap \mathcal{F}_h^{\text{time}}} \beta, \\ \alpha_{\text{sup}}^K &:= \text{ess sup}_{\partial K \cap (\mathcal{F}_h^{\text{time}} \cup \mathcal{F}_h^{\text{D}})} \alpha, & \beta_{\text{sup}}^K &:= \text{ess sup}_{\partial K \cap \mathcal{F}_h^{\text{time}}} \beta, \\ a_K &:= \max \left\{ (\alpha_{\text{sup}}^K)^{1/2}, (\beta_{\text{inf}}^K)^{-1/2} \right\}, & b_K &:= \max \left\{ (\alpha_{\text{inf}}^K)^{-1/2}, (\beta_{\text{sup}}^K)^{1/2} \right\}. \end{aligned}$$

The factor 3 appearing in the bound of Proposition 4.10 is due to the integral terms with arguments $\llbracket w \rrbracket_t^2 + (w^-)^2$ on $\mathcal{F}_h^{\text{space}}$, $\alpha \llbracket [w]_{\mathbf{N}} \rrbracket^2 + \beta^{-1} \{\{w\}\}^2$ and $\beta \llbracket \nabla w \rrbracket_{\mathbf{N}}^2 + \alpha^{-1} \|\{\{\nabla w\}\}\|^2$ on $\mathcal{F}_h^{\text{time}}$ in the definition (3.2) of the $||| \cdot |||_{\text{DG}}$ norm.

Theorem 4.11 provides the error estimate for the Trefftz-DG approximation of (1.1) in the $||| \cdot |||_{\text{DG}}$ norm assuming that Condition 4.4 holds true. It is consequence of Propositions 4.6 and 4.10, Theorem 3.4 and the ‘‘local quasi-uniformity in space’’ assumption on the mesh.

THEOREM 4.11. Let $p \in \mathbb{N}$. Let $\psi \in \mathbf{T}(\mathcal{T}_h) \cap H^{p+1}(\mathcal{T}_h)$ be the exact solution of (1.1) and $\psi_{hp} \in \mathbb{T}_p(\mathcal{T}_h)$ be the Trefftz-DG approximation solving (2.3) with $\mathbb{T}_p(\mathcal{T}_h)$ satisfying Condition 4.4 for all $K \in \mathcal{T}_h(Q)$. Set the stabilization parameters as

$$\alpha|_F = \frac{1}{h_{F_{\mathbf{x}}}} \quad \forall F \subset \mathcal{F}_h^{\text{time}} \cup \mathcal{F}_h^{\text{D}}, \quad \beta|_F = h_{F_{\mathbf{x}}} \quad \forall F \subset \mathcal{F}_h^{\text{time}}, \text{ where}$$

$$\text{for } F \subset \partial K \cap \mathcal{F}_h^{\text{D}} : \quad h_{F_{\mathbf{x}}} = h_{K_{\mathbf{x}}}$$

$$\text{for } F = K_{\mathbf{x}}^1 \times (t_{n-1}, t_n) \cap K_{\mathbf{x}}^2 \times (t_{n-1}, t_n) \subset \mathcal{F}_h^{\text{time}} :$$

$$h_{F_{\mathbf{x}}} \text{ is any constant satisfying: } \min\{h_{K_{\mathbf{x}}^1}, h_{K_{\mathbf{x}}^2}\} \leq h_{F_{\mathbf{x}}} \leq \max\{h_{K_{\mathbf{x}}^1}, h_{K_{\mathbf{x}}^2}\}.$$

Then there exists a constant C independent on the mesh size such that

$$|||\psi - \psi_{hp}|||_{\text{DG}} \leq C \sum_{K = K_{\mathbf{x}} \times (t_{n-1}, t_n) \in \mathcal{T}_h(Q)} \max\{h_{K_{\mathbf{x}}}, h_n\}^p \|\psi\|_{H^{p+1}(K)}.$$

Remark 4.12. The last formula in Remark 3.6 shows that, if $g_{\text{D}} = 0$ and the assumptions of Theorem 4.11 are satisfied, the energy dissipated by the Trefftz DG method (i.e. $\mathcal{E}(0; \psi_0) - \mathcal{E}(T, \psi_{hp})$) converges to zero proportionally to the square of the error in the DG norm, i.e. as $\max_{K \in \mathcal{T}_h(Q)} \max\{h_{K_{\mathbf{x}}}, h_n\}^{2p}$.

Remark 4.13. The previous sections show that for $d = 1, 2$ the local space $\mathbb{T}^p(K)$ has dimension $\mathcal{O}_{p \rightarrow \infty}(p^d)$ and approximates Schrödinger solutions with the same rates of the space $\mathbb{P}^p(K)$ of the degree- p polynomials on K , which has larger dimension

$\dim \mathbb{P}^p(K) = \mathcal{O}_{p \rightarrow \infty}(p^{d+1})$. More precisely, $\mathbb{T}^p(K)$ has the dimension of the space of the harmonic polynomials of degree p on K . We expect the same to hold for $d > 2$. This is a major advantage of the Trefftz approach: it achieves the same convergence rates of standard methods with considerably fewer degrees of freedom. The same situation is well-known for other PDEs, see e.g. [22], [24, Fig. 4], [17, Rem. 4.11].

5. Numerical experiments. We present some numerical experiments validating the error estimates in the mesh-dependent norm $\|\cdot\|_{\text{DG}}$ derived in [Subsection 4.5](#). We also numerically assess the error behavior with respect to $h := \max\{h_{\mathbf{x}}, h_t\}$ in the final-time, mesh-independent $\|\cdot\|_{L_2(\mathcal{F}_h^T)}$ norm and evaluate the energy dissipation of the proposed method. All experiments have been implemented in Matlab.

A direct implementation of the variational problem (2.3) leads to a large global linear system involving all the degrees of freedom of the expansion coefficients of ψ_{hp} in the basis of $\mathbb{T}_p(\mathcal{T}_h)$, over the full space–time cylinder Q . Due to the choice of the upwind-in-time numerical flux $\widehat{\psi}_{hp} = \psi_{hp}^-$ on $\mathcal{F}_h^{\text{space}}$, this system can be decomposed as a sequence of N smaller linear systems: each of them arises from solving sequentially for ψ_{hp} in each time-slab $\Omega \times [t_{n-1}, t_n]$, and using the trace of the solution from the previous slab as initial datum.

Furthermore, by choosing the same space mesh $\mathcal{T}_{h_{\mathbf{x},n}}^{\mathbf{x}}$ and time step $\tau = t_n - t_{n-1}$ for all $n = 1, \dots, N$, we can apply a time translation for each time-slab $\Omega \times [t_{n-1}, t_n]$ in the definition of the basis functions (4.1), as $\phi_\ell(\mathbf{x}, t) := \exp[i(k_\ell \mathbf{d}_\ell^\top \mathbf{x} - (k_\ell^2 + V|_K)(t - t_{n-1}))]$. This makes the matrices of the linear systems for all the time-slabs to be the same, which represents a substantial reduction in the computational cost of the method. To solve these systems we perform the LU factorization of such matrix once using the Matlab’s function `lu` with scaling and row–column permutations, which produces sparser and stable factorizations; then we solve for each time slab applying forward and backward substitutions.

As it is usual for plane-wave approximations [15, §4.3], the time-stepping matrix is ill-conditioned. We observe $\mathcal{O}(h^{-(2p+1)})$ growth of the 2-condition number κ_2 under uniform space–time mesh refinement for both the $(1+1)$ - and the $(2+1)$ -dimensional cases. A theoretical study of this matter as well as suitable preconditioning (or condition-number reduction) techniques for this method is highly relevant and will be the subject of future work.

The stabilization parameters α and β are taken as in [Theorem 4.11](#) with $h_{F_{\mathbf{x}}} = \min\{h_{K_x^1}, h_{K_x^2}\}$ for the faces in $\mathcal{F}_h^{\text{time}}$. The integrals in the assembly of the Galerkin matrix and load vectors are computed with Gauss–Legendre quadratures (combined with the Duffy transform for the integrals over triangles).

On polytopic meshes, thanks to the choice of exponential basis functions (4.1), closed formulas for all the integrals appearing in the matrix assembly could be written, following the ideas in [15, §4.1]. We recall that the Trefftz-DG formulation (2.3) does not involve $(d+1)$ -dimensional integrals over mesh elements but only on the d -dimensional element faces.

5.1. Square potential well in 1 + 1 dimensions. Let us consider the $(1+1)$ -dimensional Schrödinger equation (1.1) on $Q = (-2, 2) \times (0, 1)$ with homogeneous Dirichlet boundary conditions and the following square-well potential:

$$(5.1) \quad V(x) = \begin{cases} 0, & x \in (-1, 1), \\ V_*, & x \in (-2, 2) \setminus (-1, 1), \end{cases}$$

for some $V_* > 0$. The initial condition is taken as an eigenfunction (bound state) of $-\partial_x^2 + V$ on $(-2, 2)$:

$$\psi_0(x) = \begin{cases} \cos(k_*x), & x \in (-1, 1), \\ \frac{\cos(k_*)}{\sinh(\sqrt{V_* - k_*^2})} \sinh(\sqrt{V_* - k_*^2}(2 - |x|)), & x \in (-2, 2) \setminus (-1, 1), \end{cases}$$

where k_* is a real root of the function $f(k) := \sqrt{V_* - k^2} - k \tan(k) \tanh(\sqrt{V_* - k^2})$. The solution of the corresponding initial boundary value problem (1.1) is $\psi(x, t) = \psi_0(x) \exp(-ik^2t)$. For each V_* there is a finite number of such values k_* : in the numerical experiments below we take the largest one, corresponding to faster oscillations in space and time. In Figure 5 we present the plot the function $f(x)$ for $V_* = 20$ and $V_* = 50$ with the values of k_* used in this experiment.

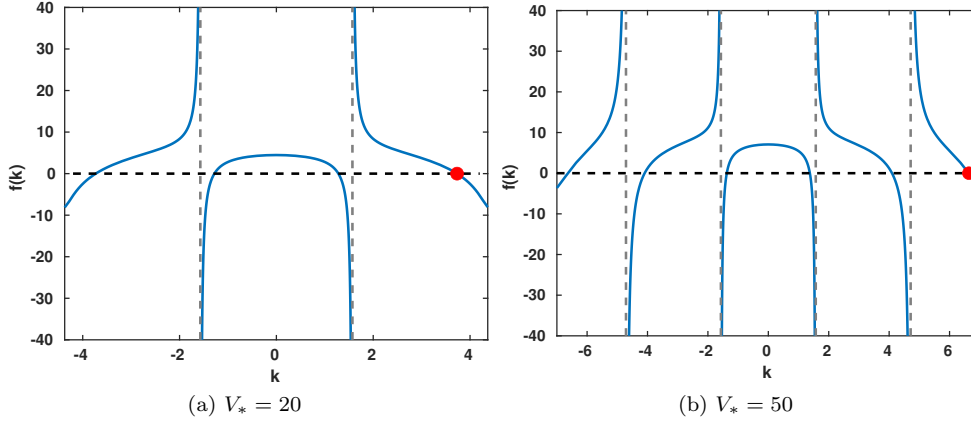


Fig. 5: Plot of $f(k)$ for different values of V_* . The red dots are the values of k taken in the numerical experiments: $k_* \approx 3.7319$ ($V_* = 20$) and $k_* \approx 6.6394$ ($V_* = 50$).

From the definition (4.12) of the Trefftz basis, we observe that if the parameters k_ℓ are chosen very close to one another then the corresponding basis functions approach mutual linear dependence. The consequence is that the Trefftz-DG method becomes more and more ill-conditioned. This is confirmed by the Vandermonde-like matrix \mathbf{V} in (4.16), which is singular in the limit $|k_{\ell_1} - k_{\ell_2}| \rightarrow 0$. In the experiments we take $2p + 1$ equally spaced values $k_\ell \in \{-p, -(p-1), \dots, 0, \dots, p-1, p\}$.

In Figures 6a and 6b we plot the Trefftz-DG numerical approximations ψ_{hp} obtained for $p = 3$ on the finest mesh (described below) with $V_* = 20$ and $V_* = 50$ respectively. It can be observed that for increasing V_* the solution oscillates more with respect to x in $(-1, 1)$, while it decays monotonically to 0 in $(-2, 2) \setminus (-1, 1)$.

In Figure 7a we plot the DG norm of the Galerkin error obtained for $V_* = 20$ and a sequence of space-time, uniform, Cartesian meshes with $h_x = 0.2, 0.1, 0.0667, 0.05$, $h_t = 0.25h_x$ and $p = 1, 2, 3$.

Since we have homogeneous Dirichlet boundary conditions, the continuous model preserves the energy functional $\mathcal{E}(t, \psi)$, recall Remark 3.6. In Figure 8a we show the time-evolution of the energy error for the Trefftz-DG approximation for the finest mesh, which is smaller for larger p , as expected. Moreover, in Figure 8b we numerically observe that \mathcal{E}_{loss} converges to zero as $\mathcal{O}(h^{2p})$, as it can be proved combining

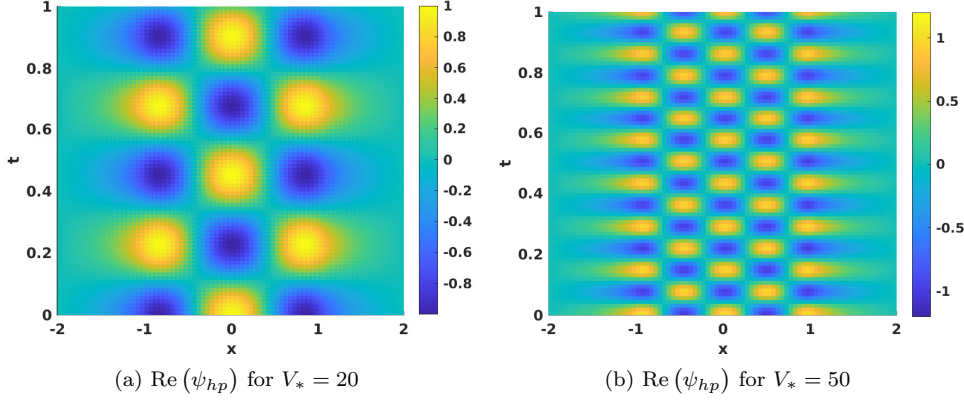


Fig. 6: Trefftz-DG approximation ψ_{hp} in the space-time cylinder Q for the $(1+1)$ -dimensional square-well potential problem (5.1) computed with $p = 3$.

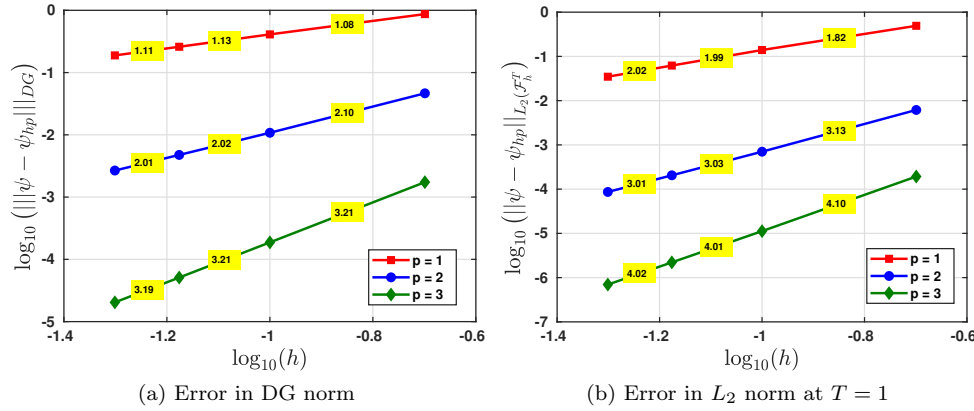


Fig. 7: Trefftz-DG error for the $(1+1)$ -dimensional problem with square well potential (5.1) with $V_* = 20$. The numbers in the yellow rectangles are the empirical algebraic convergence rates in h .

Theorem 4.11 and Remark 3.6.

In order to see the effect of the choice of the parameters k_ℓ , we first note that in this experiment we know the time frequency of the exact solution, which is $\omega = k_*^2$. Therefore it is natural to expect the approximation to be better if our basis functions oscillates at the same time frequency. To numerically illustrate this, in Figures 9a and 9b we show that the convergence rates clearly degrade for $p = 1$, $V_* = 50$ and $V_* = 100$, and our previous choice of the parameters k_ℓ , as the time frequencies of the basis functions are too far from those of the exact solution. On the contrary, by taking the parameters k_ℓ as $\{-k_*, 0, k_*\}$ we recover the expected rates. This clearly suggests that a sensible tuning of the basis function parameters can significantly improve the accuracy of the method.

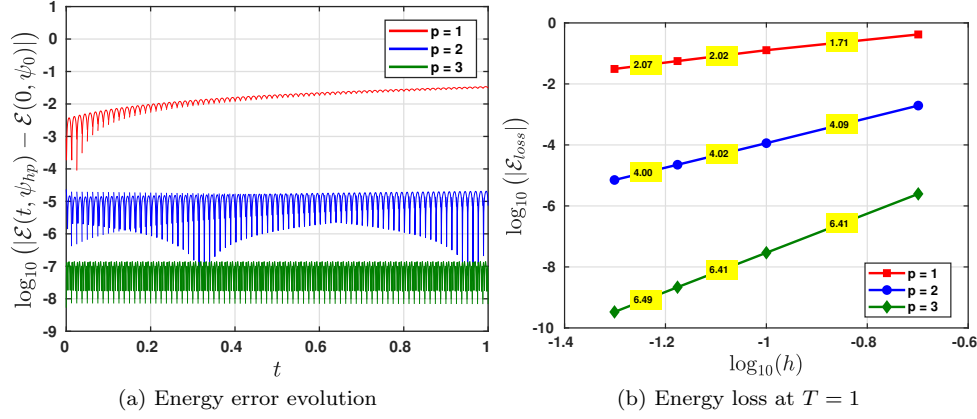


Fig. 8: Time-evolution of the energy error and dependence on h and p for the problem with square-well potential and $V_* = 20$.

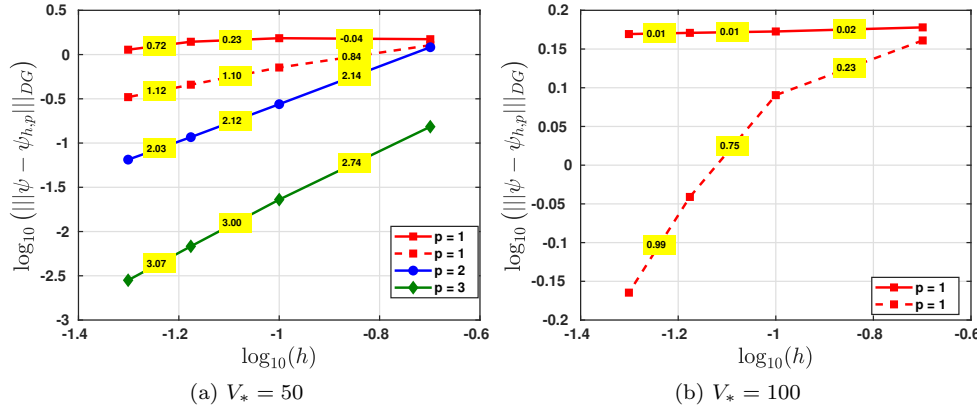


Fig. 9: Trefftz-DG error measured in DG norm for the (1 + 1) dimensional problem with square-well potential (5.1) with $V_* = 50$ ($k_* \approx 6.6394$) and $V_* = 100$ ($k_* \approx 9.6812$), and for $k_\ell \in \{-p, \dots, p\}$ (continuous line), which is the same choice of the previous plots, and $k_\ell \in \{0, \pm k_*\}$ (dashed line).

5.2. (2+1)-dimensional transient Gaussian distribution. We consider the linear Schrödinger equation (1.1) with zero potential $V = 0$ on $Q = \Omega \times (0, 2)$, with $\Omega = (-2, 4) \times (-2.5, 2.5)$. Following [2], the initial and boundary conditions are chosen such that the exact solution is

$$\psi(x, y, t) = \frac{i}{i - 4t} e^{-\frac{i}{i-4t}(x^2 + y^2 + ix + it)}.$$

The basis function parameters are chosen as $p + 1$ equally spaced space wavenumbers $k_m = 1, 2, \dots, p + 1$, and the equally spaced angles $\theta_{m,\lambda} = \frac{2\pi(\lambda-1)}{2m+1}$ in $(0, 2\pi]$, $\lambda = 1, \dots, 2m + 1$, as in Figure 3.

In Figure 10a we show the convergence rates of the Trefftz-DG approximation

for a set of structured triangular meshes generated by halving each rectangle in a Cartesian partition of Ω with equal number of divisions (20, 40, 60, 80) in both x and y directions. In this experiment $h_t \approx 0.5h_x$. The $\mathcal{O}(h^p)$ convergence rates obtained are in agreement with [Theorem 4.11](#). Similarly to the (1+1)-dimensional example in the previous section, in [Figure 10b](#) we observe $\mathcal{O}(h^{p+1})$ convergence rates in the $L_2(\Omega)$ norm at the final time. Not shown here, similar results were obtained for rectangular meshes in space.

In [Figure 11](#) we study the p -convergence of the method: for the two coarsest space meshes with $h_t \approx h_x/8$, and for $p \in \{1, 2, 3, 4\}$, the DG norm of the error is plotted against the total number of degrees of freedom in Q . We observe $\mathcal{O}(e^{-b\sqrt{\#\text{DOF}}})$ convergence when the “local degree” p is raised. This is in strong contrast with what one might expect from a polynomial method: in that case only the slower rate $\mathcal{O}(e^{-b\sqrt[3]{\#\text{DOF}}})$ can be achieved (recall [Remark 4.13](#)). The Trefftz-DG approximations for $p = 3$, at the initial and final times, are shown in [Figure 12](#).

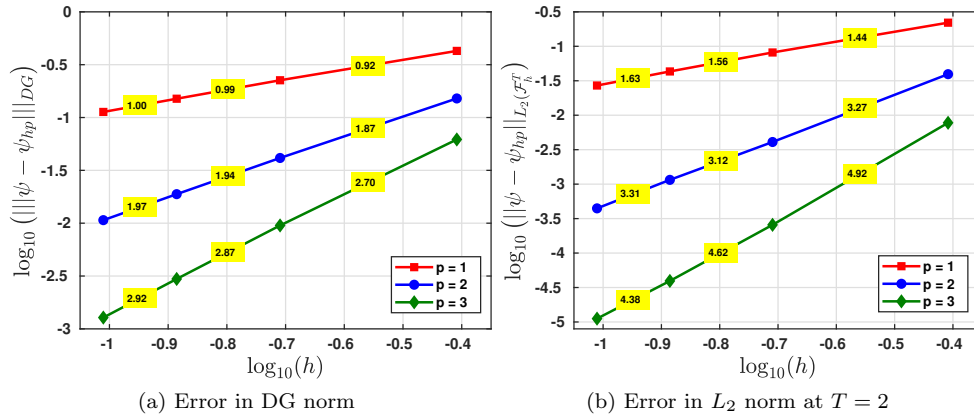


Fig. 10: Trefftz-DG error for the (2+1)-dimensional transient Gaussian problem.

6. Concluding remarks. We have introduced a Trefftz DG method for the approximation of the time-dependent, linear Schrödinger equation. We have analysed its well-posedness, stability and h -convergence properties. As this is the first description of such a numerical scheme, several extensions and improvements of the method and its analysis might be addressed. We list here a few possible future research directions.

- The extension of the h -convergence bounds to space dimensions higher than 2.
- The proof of optimal error estimates in mesh-independent norms such as $L^2(Q)$ (cf. the duality approach used in [23, §5.4] for the wave equation).
- The analysis of the method in locally refined space–time meshes, as in [23].
- The p -convergence analysis, i.e. the proof of convergence rates for sequences of discrete spaces obtained by local enrichment on a fixed mesh (the Trefftz equivalent of increasing the local polynomial degrees). Only the best-approximation bounds are missing, as the quasi-optimality bound (3.6) is independent of the discrete space. This is a very challenging task, given the nature of the Trefftz basis functions. In fact, this was accomplished for the Helmholtz equation [22] but not yet for the wave equation.
- The “sparsification” of the scheme, i.e. the combination with sparse-grid tech-

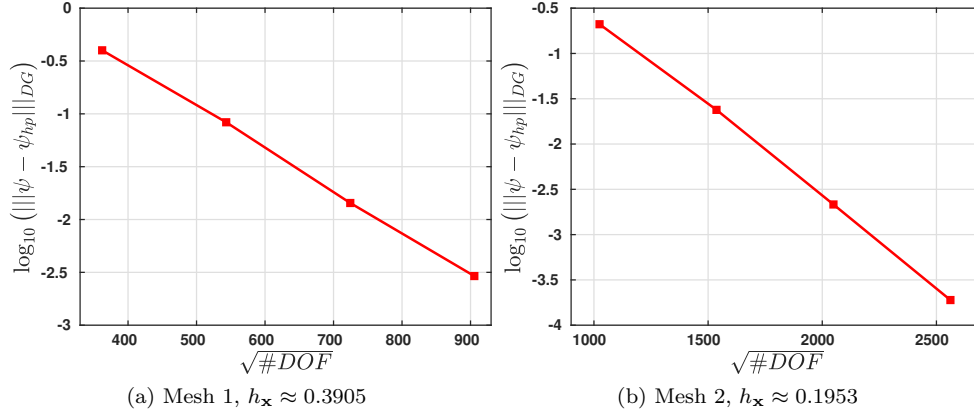


Fig. 11: p -convergence of the Trefftz-DG error against the squared root of the total number of degrees of freedom for the $(2+1)$ -dimensional transient Gaussian problem.

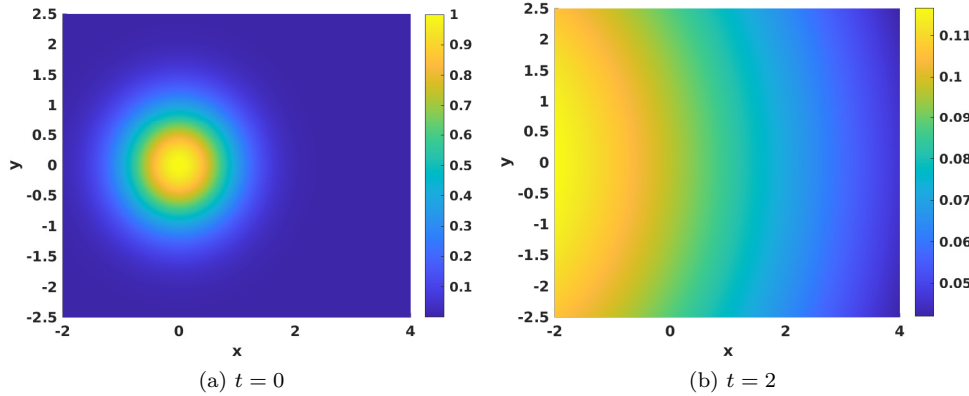


Fig. 12: Trefftz-DG approximation of the $(2+1)$ -dimensional transient Gaussian.

niques in space-time to improve its efficiency, e.g. along the lines of [4].

- The extension to non-piecewise-constant potentials V , in particular to smooth potentials that are relevant for applications (e.g. Coulomb-interaction potentials in quantum mechanics). Useful tools towards this goal are the “generalized plane waves” developed for the Helmholtz equation in [16] and subsequent papers, and the closely related “quasi-Trefftz” approach developed for the wave equation in [17].
- Efficient implementations, e.g. using the closed-form integration of [15, §4.1].
- A more accurate analysis of the Trefftz discrete spaces in order to optimise the choice of the parameters (k_ℓ and \mathbf{d}_ℓ in (4.1)), improving conditioning, robustness and accuracy. Basis different from complex exponentials might also be devised and analysed. The poor conditioning of the time-stepping matrix is likely to be the main bottleneck for the use of the proposed scheme

in demanding applications: the Trefftz technologies recently developed for time-harmonic wave problems might greatly help under this respect.

- The extension to initial boundary value problems with non-reflecting boundary conditions, which are often used to truncate unbounded domains (e.g. [2]). Under this respect the Trefftz approach is promising as it allows the selection of outward-propagating basis functions on boundary cells, as in [10].

REFERENCES

- [1] D. R. Adams and L. I. Hedberg. *Function spaces and potential theory*, volume 314 of *Grundlehren der Mathematischen Wissenschaften*. Springer-Verlag, Berlin, 1996.
- [2] X. Antoine, C. Besse, and V. Mouysset. Numerical schemes for the simulation of the two-dimensional Schrödinger equation using non-reflecting boundary conditions. *Math. Comp.*, 73(248):1779–1799, 2004.
- [3] L. Banjai, E. Georgoulis, and O. Lijoka. A Trefftz polynomial space-time discontinuous Galerkin method for the second order wave equation. *SIAM J. Num. Anal.*, 55(1):63–86, 2017.
- [4] P. Bansal, A. Moiola, I. Perugia, and C. Schwab. Space-time discontinuous Galerkin approximation of acoustic waves with point singularities. *IMA J. Numer. Anal.*, 12 2020.
- [5] S. Brenner and R. Scott. *The mathematical theory of finite element methods*, volume 15. Springer Science & Business Media, 2007.
- [6] J. Callahan. *Advanced calculus: a geometric view*. Springer Science & Business Media, 2010.
- [7] O. Cessenat and B. Despres. Application of an ultra weak variational formulation of elliptic PDEs to the two-dimensional Helmholtz problem. *SIAM J. Num. Anal.*, 35(1):255–299, 1998.
- [8] R. Durán. On polynomial approximation in Sobolev spaces. *SIAM J. Num. Anal.*, 20(5):985–988, 1983.
- [9] H. Egger, F. Kretzschmar, S. Schnepf, and T. Weiland. A space-time discontinuous Galerkin Trefftz method for time dependent Maxwell’s equations. *SIAM J. Sci. Comput.*, 37(5):B689–B711, 2015.
- [10] H. Egger, F. Kretzschmar, S.M. Schnepf, I. Tsukerman, and T. Weiland. Transparent boundary conditions for a discontinuous Galerkin Trefftz method. *Appl. Math. Comput.*, 267:42–55, 2015.
- [11] C. Gittelsohn, R. Hiptmair, and I. Perugia. Plane wave discontinuous Galerkin methods: analysis of the h-version. *ESAIM: Math. Model. and Num. Anal.*, 43(2):297–331, 2009.
- [12] R. Grella. Fresnel propagation and diffraction and paraxial wave equation. *J. of Optics*, 13(6):367, 1982.
- [13] N. J. Higham. *Accuracy and stability of numerical algorithms*. Society for Industrial and Applied Mathematics (SIAM), Philadelphia, PA, second edition, 2002.
- [14] R. Hiptmair, A. Moiola, and I. Perugia. Error analysis of Trefftz-discontinuous Galerkin methods for the time-harmonic Maxwell equations. *Math. Comp.*, 82(281):247–268, 2013.
- [15] R. Hiptmair, A. Moiola, and I. Perugia. A survey of Trefftz methods for the Helmholtz equation. In *Building bridges: connections and challenges in modern approaches to numerical partial differential equations*, pages 237–279. Springer, 2016.
- [16] L.-M. Imbert-Gérard and B. Després. A generalized plane-wave numerical method for smooth nonconstant coefficients. *IMA J. Numer. Anal.*, 34(3):1072–1103, 2014.
- [17] L.-M. Imbert-Gérard, A. Moiola, and P. Stocker. A space-time quasi-trefftz dg method for the wave equation with piecewise-smooth coefficients. *arXiv preprint arXiv:2011.04617*, 2020.
- [18] J. Keller and J. Papadakis. *Wave propagation and underwater acoustics*. Springer, 1977.
- [19] E. Lifshitz and Landau L. *Quantum Mechanics; Non-relativistic Theory*. Pergamon Press, 1965.
- [20] J.-L. Lions and E. Magenes. *Non-homogeneous boundary value problems and applications. Vol. I*. Springer-Verlag, New York-Heidelberg, 1972.
- [21] W. McLean. *Strongly elliptic systems and boundary integral equations*. Cambridge University Press, Cambridge, 2000.
- [22] A. Moiola, R. Hiptmair, and I. Perugia. Plane wave approximation of homogeneous Helmholtz solutions. *Z. Angew. Math. Phys.*, 62(5):809–837, 2011.
- [23] A. Moiola and I. Perugia. A space-time Trefftz discontinuous Galerkin method for the acoustic wave equation in first-order formulation. *Numer. Math.*, 138(2):389–435, 2018.
- [24] I. Perugia, J. Schöberl, P. Stocker, and C. Wintersteiger. Tent pitching and Trefftz-DG method for the acoustic wave equation. *Comput. Math. Appl.*, 79(10):2987–3000, 2020.